

Supplemental Data

Defining Network Topologies that Can Achieve Biochemical Adaptation

Wenzhe Ma, Ala Trusina, Hana El-Samad, Wendell Lim, and Chao Tang

Supplemental Experimental Procedures

1. Selection criteria for functional performance

In the Experimental Procedure of the main text, we have described the mathematical definition of the functional performance (see also Figure S5, OUTPUT I) and the criteria for discarding certain “ill-behaved” circuits. In particular, the circuit is discarded if there is a sustained oscillation. If the oscillation is under-damped, the circuit may still eventually adapt. However, too large a swing in the output may compromise the functionality of adaptation. We chose to set a criterion to discard those circuits with large swings, even they may adapt eventually. Specifically, in case of under-damped oscillation, we monitored two values shown in Figure S5 (OUTPUT II): the height of the first peak relative to the initial steady state, O_{peak1} and the height of the second peak, also relative to the initial steady state, O_{peak2} . The circuit is discarded from the functional map unless the first peak is larger than twice of the second one, i.e. $O_{\text{peak1}} > 2O_{\text{peak2}}$.

2. Comparison of negative feedback loops with and without buffer node

One of our main results is that a negative feedback loop with a buffer node is capable of perfect adaptation while a negative feedback loop without a buffer node is not (see Figure 2A). Here we use two examples to further illustrate the importance of the buffer node in achieving perfect

adaptation. Both of the example networks are 3 node networks with a single negative feedback loop (Figure S6). The first network has the loop go through the nodes in the order ACBA (Figure S6, upper panel). In this case, the output node C first goes to the regulator node B, which in turn feeds back to the input node A. The second network has the loop go in the order ABCA (Figure S6, lower panel). In this case, the output node C directly feeds back to the input node A. The corresponding phase space and nullcline of the two networks are also shown in Figure S6. For the first network, which is capable of perfect adaptation, the B -nullcline (black line) is unchanged while the C -nullcline (red lines) moves horizontally with the change of input. For the second network, the situation is reversed: the C -nullcline (black line) does not move while the B -nullcline (red lines) moves vertically in response to the input change. The steady state values B^* and C^* are determined by the intersection of the black and red nullclines. For the first network, the C^* changes little (if the B -nullcline is flat enough) while B^* changes considerably with respect to the input change. On the contrary, for the second network C^* changes considerably corresponding to the input change while B^* does not change much. We see that the roles of Node B and Node C are exchanged in the two networks. This can also be seen from their kinetic equations: the equations for the second network are the same as for the first one if we rename the node B as C and C as B. So in the second network, Node C becomes the buffer node. Because we fix our output on the node C, the relative position of the nodes on the negative feedback loop is important.

3. The incoherent feed-forward loop in which A and B acting on C with the same sign

With A and B acting on Node C with the same sign (positive or negative), A represses B would make an incoherent feed-forward loop. This kind of incoherent feed-forward loop cannot achieve

perfect adaptation. For the example shown in Figure 2B (bottom panel), with both A and B positively regulating C, the kinetic equations are:

$$\begin{aligned}\frac{dA}{dt} &= Ik_{IA} \frac{(1-A)}{(1-A)+K_{IA}} - F_A k'_{F_AA} \frac{A}{A+K'_{F_AA}}, \\ \frac{dB}{dt} &= E_B k_{E_BB} \frac{(1-B)}{(1-B)+K_{E_BB}} - Ak'_{AB} \frac{B}{B+K'_{AB}}, \\ \frac{dC}{dt} &= Ak_{AC} \frac{(1-C)}{(1-C)+K_{AC}} + Bk_{BC} \frac{(1-C)}{(1-C)+K_{BC}} - F_C k'_{F_CC} \frac{C}{C+K'_{F_CC}}.\end{aligned}\tag{S1}$$

To have perfect adaptation, C^* must be independent of both A^* and B^* . From the third equation in Eq. (S1) in which the first two terms are both positive, we see that it is impossible to have A^* and B^* both disappear from the steady state equation for C in any way that is robust.

4. Motif analysis of the 395 adaptation networks

The 395 adaptation networks are randomized to serve as the NULL space. Specifically, we randomly select two networks among the 395 networks and exchange their links at a randomly selected position (e.g. A to B) if and only if there is a link in both networks at this position. 1000 randomized ensembles of 395 networks are generated in this way. The average number of appearance \bar{f} and the standard deviation d of each motif in these ensembles are then obtained.

The “Motif over-representation” in Figure 4 is defined as $(f - \bar{f})/d$, where f is the number of appearance of the motif in the 395 adaptation networks.

In order to find any commonalities among these 395 overrepresented robust topologies for adaptation, we first searched for over-represented motifs (Figure S7) in these networks. We used all the 2-node and 3-node feedback and feed-forward loops as motifs, and compared their frequency of appearance in the 395 adaptation topologies with ensembles of randomized networks (Experimental Procedures). The results clearly indicate that specific negative feedback

loops and some incoherent feed-forward loops are over-represented. The common feature for most over-represented negative feedback loops is that they lack a link in which the output node C directly feeds back on the input node A. The common feature of the most over-represented incoherent feed-forward loops is that the node C is regulated by the nodes A and B with opposing signs. These observations for the entire architecture space are consistent with our previous observations gleaned from analysis of minimal circuits – the minimal architectures that are sufficient for adaptation are all overrepresented within the best complex architectures capable of adaptation.

5. Analysis of NFBLB class with positive self-loop on B

We found that a subset of NFBLB class of adaptation networks have a positive self-loop on the buffer node B. This type of topology achieves perfect adaptation with a similar geometric interpretation as in the NFBLB topologies without this positive loop, i.e. a flat B -nullcline near the steady states (Figure S8). However, in contrast to those NFBLB topologies without the positive self-loop, here the flat B -nullcline is accomplished through a very different mechanism than ultrasensitivity. This can be easily gleaned from the updated equations for B , reflecting the auto-regulation (Figure S8):

$$\frac{dB}{dt} = B k_{BB} \frac{(1-B)}{(1-B) + K_{BB}} - C k'_{CB} \frac{B}{B + K'_{CB}}. \quad (\text{S2})$$

We can have a steady state C^* that is independent of B^* if $(1-B) \gg K_{BB}$ and $B \ll K'_{CB}$. Under these conditions, Eq. (S2) can be approximated as

$$\frac{dB}{dt} = B k_{BB} - C k'_{CB} \frac{B}{K'_{CB}} = B \frac{k'_{CB}}{K'_{CB}} (C^* - C), \quad (\text{S3})$$

where $C^* = k_{BB} K'_{CB} / k'_{CB}$. Thus, when the auto regulation loop works in the saturated region and the negative regulation from C to B works in the linear region, this topology can achieve perfect adaptation (and in this case the B -nullcline is perfectly flat). Here it is the logarithm of B , instead of B itself, that integrates the adaptation error. To see this, rewrite Eq. (S3) as $d \ln B / dt = k'_{CB} (C^* - C) / K'_{CB}$. So $\text{Log}(B)$ is the integrator and $B = B^*(I_0) e^{(k'_{CB} / K'_{CB}) \int_0^t (C^* - C) d\tau}$ feedbacks to Node C. This seems to be a special form of the integral control. Figure S8 illustrated the effect of the key parameters to the adaptation precision. Expectedly, high adaptation precision is achieved by letting the two key parameters go to the required limits and large sensitivity is achieved through the separation of time scales between the response time and the recovery time of Node C.

6. Theoretic analysis for the classification of all adaptation circuits

In the next two sections, we present a general analysis for conditions leading to perfect adaptation. The end products of this analysis are: (1) all 3-node circuits that are capable of perfect adaptation fall into two topological classes, NFBLB and IFFLP; and (2) the control node B plays a defined role in each class with a set of regulation menu.

6.1 General formulation

For 3-node networks, the general kinetic equations are:

$$\left\{ \begin{array}{l} \frac{dA}{dt} = f_A = k_{IA} I \frac{1-A}{1-A+K_{IA}} + \sum_i k_{X_i A} X_i \frac{1-A}{1-A+K_{X_i A}} - \sum_i k'_{Y_i A} Y_i \frac{A}{A+K'_{Y_i A}} \\ \frac{dB}{dt} = f_B = \sum_i k_{X_i B} X_i \frac{1-B}{1-B+K_{X_i B}} - \sum_i k'_{Y_i B} Y_i \frac{B}{B+K'_{Y_i B}} \\ \frac{dC}{dt} = f_C = \sum_i k_{X_i C} X_i \frac{1-C}{1-C+K_{X_i C}} - \sum_i k'_{Y_i C} Y_i \frac{C}{C+K'_{Y_i C}} \end{array} \right. \quad (\text{S4})$$

where $X_i = A, B, C, E_A, E_B$ or E_C are activating enzymes and $Y_i = A, B, C, F_A, F_B$ or F_C are deactivating enzymes. Expanding Eq. (S4) around the steady state (A^*, B^*, C^*) , the linearized equations are:

$$\begin{aligned} \begin{bmatrix} \frac{d\Delta A}{dt} \\ \frac{d\Delta B}{dt} \\ \frac{d\Delta C}{dt} \end{bmatrix} &= \begin{bmatrix} \frac{\partial f_A}{\partial A} & \frac{\partial f_A}{\partial B} & \frac{\partial f_A}{\partial C} \\ \frac{\partial f_B}{\partial A} & \frac{\partial f_B}{\partial B} & \frac{\partial f_B}{\partial C} \\ \frac{\partial f_C}{\partial A} & \frac{\partial f_C}{\partial B} & \frac{\partial f_C}{\partial C} \end{bmatrix} \begin{bmatrix} \Delta A \\ \Delta B \\ \Delta C \end{bmatrix} + \begin{bmatrix} \frac{\partial f_A}{\partial I} \\ 0 \\ 0 \end{bmatrix} \Delta I \\ &\equiv \begin{bmatrix} \alpha_{AA} & \beta_{BA} & \beta_{CA} \\ \beta_{AB} & \alpha_{BB} & \beta_{CB} \\ \beta_{AC} & \beta_{BC} & \alpha_{CC} \end{bmatrix} \begin{bmatrix} \Delta A \\ \Delta B \\ \Delta C \end{bmatrix} + \begin{bmatrix} \frac{\partial f_A}{\partial I} \\ 0 \\ 0 \end{bmatrix} \Delta I \end{aligned} \quad (\text{S5})$$

It is easy to show that if there is no positive self-regulation on the node i , the corresponding α_{ii} is always negative. α_{ii} can only be positive for special parameter sets with positive self-regulation. The sign of β_{ij} depends solely on the sign of regulation. For example β_{BA} is positive, negative, or zero if the regulation from B to A is positive, negative, or absent. Since we defined the input as activating, $\frac{\partial f_A}{\partial I}$ is always a nonzero positive number.

At steady state,

$$\begin{bmatrix} \Delta A^* \\ \Delta B^* \\ \Delta C^* \end{bmatrix} = - \begin{bmatrix} \alpha_{AA} & \beta_{BA} & \beta_{CA} \\ \beta_{AB} & \alpha_{BB} & \beta_{CB} \\ \beta_{AC} & \beta_{BC} & \alpha_{CC} \end{bmatrix}^{-1} \begin{bmatrix} \frac{\partial f_A}{\partial I} \\ 0 \\ 0 \end{bmatrix} \Delta I. \quad (\text{S6})$$

The relative adaptation error can be captured by the following equation:

$$\frac{\Delta C^*/C^*}{\Delta I/I} = \frac{I}{C^*} \frac{\partial f_A}{\partial I} \left(\begin{bmatrix} \alpha_{AA} & \beta_{BA} & \beta_{CA} \\ \beta_{AB} & \alpha_{BB} & \beta_{CB} \\ \beta_{AC} & \beta_{BC} & \alpha_{CC} \end{bmatrix}^{-1} \right)_{31} = \frac{I}{C^*} \frac{\partial f_A}{\partial I} \frac{M_{13}}{J}. \quad (\text{S7})$$

where

$$M_{13} = \begin{vmatrix} \beta_{AB} & \alpha_{BB} \\ \beta_{AC} & \beta_{BC} \end{vmatrix} = \beta_{AB}\beta_{BC} - \alpha_{BB}\beta_{AC} \quad (\text{S8})$$

is the (1,3) minor of the Jacobian matrix, and

$$\begin{aligned} J &= \begin{vmatrix} \alpha_{AA} & \beta_{BA} & \beta_{CA} \\ \beta_{AB} & \alpha_{BB} & \beta_{CB} \\ \beta_{AC} & \beta_{BC} & \alpha_{CC} \end{vmatrix} \\ &= \alpha_{AA}\alpha_{BB}\alpha_{CC} + \beta_{BA}\beta_{AC}\beta_{CB} + \beta_{CA}\beta_{AB}\beta_{BC} - \alpha_{AA}\beta_{CB}\beta_{BC} - \alpha_{BB}\beta_{CA}\beta_{AC} - \alpha_{CC}\beta_{AB}\beta_{BA} \end{aligned} \quad (\text{S9})$$

is the Jacobian determinant. Perfect adaptation requires Eq. (S7) be 0. Since $\frac{\partial f_A}{\partial I}$ and I are not zero, the only possibility is to make the minor $M_{13} = 0$ while maintaining a nonzero value for the Jacobian determinant J . Furthermore, the stability of the steady state requires a negative Jacobian determinant, i.e. $J < 0$.

Let us analyze the conditions for $M_{13} = 0$. There are two terms in Eq. (S8): $\beta_{AB}\beta_{BC}$ and $\alpha_{BB}\beta_{AC}$. Thus, the condition for Eq. (S8) be zero is that either both terms are 0 ($\beta_{AB}\beta_{BC} = \alpha_{BB}\beta_{AC} = 0$ – the first category) or the two terms are equal but nonzero ($\beta_{AB}\beta_{BC} = \alpha_{BB}\beta_{AC} \neq 0$ – the second category).

NFBLB class

We show that the first category, $\beta_{AB}\beta_{BC} = \alpha_{BB}\beta_{AC} = 0$, corresponds to the adaptation networks of NFBLB class. Notice that these two terms are related with two signal pathways from Node A to Node C, respectively. The term $\beta_{AB}\beta_{BC}$ is related with the pathway $A \Rightarrow B \Rightarrow C$. $\beta_{AB}=0$ would mean that there is no $A \Rightarrow B$ link; $\beta_{BC}=0$ would mean that there is no $B \Rightarrow C$ link. $\beta_{AB}\beta_{BC}=0$ would imply that at least one of the factors is zero and at least one of the links is missing so that there is no signal going from A to C through the pathway $A \Rightarrow B \Rightarrow C$. The other term $\alpha_{BB}\beta_{AC}$ corresponds to the pathway $A \Rightarrow C$. If $\beta_{AC}=0$, $A \Rightarrow C$ is missing, so that no signal can go directly from A to C. Because at least one of the two signal pathways must exist to transmit the signal and the pathway $A \Rightarrow B \Rightarrow C$ does not exist in this case ($\beta_{AB}\beta_{BC}=0$), $A \Rightarrow C$ must be present. This implies $\beta_{AC} \neq 0$. Thus α_{BB} must be 0 to make $\alpha_{BB}\beta_{AC}=0$. Therefore, this category can be classified into two (overlapping) cases: (a) $\alpha_{BB}=0$ and $\beta_{AB}=0$ (while β_{BC} can be either nonzero or zero), (b) $\alpha_{BB}=0$ and $\beta_{BC}=0$ (while β_{AB} can be either nonzero or zero). We discuss each of these cases in the following.

(a) $\alpha_{BB}=0$ and $\beta_{AB}=0$

In this case, there is no link from A to B and the Jacobian determinant $J = \beta_{AC}\beta_{CB}\beta_{BA} - \alpha_{AA}\beta_{BC}\beta_{CB}$ (see Eq. (S9)). Note that the two terms in J correspond to two feedback loops, respectively. That is, $\beta_{AC}\beta_{CB}\beta_{BA}$ is nonzero only if every factor in it is nonzero, which implies the existence of the three links $A \Rightarrow C$, $C \Rightarrow B$, and $B \Rightarrow A$. These three links form a feedback loop $A \Rightarrow C \Rightarrow B \Rightarrow A$. Similarly, $\alpha_{AA}\beta_{BC}\beta_{CB}$ is nonzero only if there is a feedback loop $C \Rightarrow B \Rightarrow C$. Thus, a nonzero J requires that the network contain at least one of the two feedback loops. Since β_{CB} is in both of

the terms in J (the link $C \Rightarrow B$ is part of both feedback loops), $C \Rightarrow B$ must exist in this case. It is worthwhile emphasizing that in both feedback loops the output node C first goes to the intermediate node B (buffer) before feeding back either to the input node A or to the output node C .

Recall that the sign of the β_{ij} is the same as the sign of the link, e.g. if the link $A \Rightarrow C$ is negative then $\beta_{AC} < 0$, and that $\alpha_{AA} < 0$ (unless there is a positive self-loop on A – a case we will discuss in the next paragraph). The stability requirement of a negative J requires that at least one of the feedback loops is negative. Furthermore, two negative loops would make a more negative J (larger absolute value) and thus a smaller adaptation error (see Eq. (S7)) than a single negative loop. Therefore, this case of adaptation networks correspond to one or two negative feedback loops, using the node B as a buffer node.

If there is a positive self-loop on node A , α_{AA} can be positive with some parameter choices. In this case, a positive feedback loop $C \Rightarrow B \Rightarrow C$ would make the second term in J negative, i.e. $-\alpha_{AA}\beta_{BC}\beta_{CB} < 0$. However, note that $J < 0$ is necessary but not sufficient for stability. J is equal to the product of all three eigenvalues. $J < 0$ when either all of the three eigenvalues are negative (a stable steady state), or one of them is negative and the other two are positive (an unstable steady state). We can show that for the simple topology, $A \rightarrow A$ (self-positive loop), $A \Rightarrow C$ (positive or negative), $C \Rightarrow B \Rightarrow C$ (positive loop), the steady state that would otherwise achieve perfect adaptation is unstable. With one more link $C \Rightarrow A$ added to this topology so that there is a *negative* feedback loop $A \Rightarrow C \Rightarrow A$ in the network, we found that the linearized equations can achieve perfect adaptation with certain parameter choices. To see if this topology can achieve perfect adaptation with the full nonlinear kinetic equations, we performed extensive numerical

analysis and found no sign of perfect adaptation. However, we do not have a rigorous proof to exclude this network from being able to perfectly adapt.

(b) $\alpha_{BB}=0$ and $\beta_{BC}=0$

In this case, there is no link from B to C and $J = \beta_{AC}\beta_{CB}\beta_{BA} - \alpha_{CC}\beta_{AB}\beta_{BA}$. Similar to the analysis above, the circuit should contain at least one of the two negative feedback loops that go through the node B: $A \Rightarrow C \Rightarrow B \Rightarrow A$ and $A \Rightarrow B \Rightarrow A$. Again, two negative loops would in general result in a smaller adaptation error than a single loop.

IFFLP class

The second category of zero adaptation error is $\beta_{AB}\beta_{BC} = \alpha_{BB}\beta_{AC} \neq 0$ (see Eq. (S8)). Nonzero β_{AB} , β_{BC} and β_{AC} imply the existence of the links $A \Rightarrow B$, $B \Rightarrow C$ and $A \Rightarrow C$, that is, a feed-forward loop. Whether the feed-forward loop is coherent or incoherent depends on whether $\beta_{AB}\beta_{BC}/\beta_{AC} = \alpha_{BB}$ is positive or negative. If there is no positive self-loop on the node B, it is easy to show that α_{BB} is always negative. It can also be shown that if there is no feedback loops in the network (so that the Jacobian matrix is triangular) stability of the steady state requires all diagonal elements including α_{BB} be negative, which holds even with the presence of a positive self-loop on B. Thus in all these cases, the FFL leading to perfect adaptation should be incoherent.

On the other hand, there may exist some network topologies that contain a *coherent* FFL, a positive self-loop on B and at least one feedback loop that, with some special parameters, possess a *stable* steady state with $\alpha_{BB} > 0$. These topologies could achieve perfect adaption with the mechanism of IFFLP class. We will discuss one such example later.

7. The role of the control node B in perfect adaptation

In this section, we elaborate the importance of the node B in controlling the adaptation precision.

We present an analysis on the general forms of the regulation on the B-node and enumerate all possible B-regulations that can lead to perfect adaptation in both NFBLB and IFFLP classes of adaptation networks.

Let us consider the kinds of mathematical relationships that a steady state equation of enzymatic reaction kinetics can establish robustly. The general steady state equation for a node (B) is

$$\frac{dB}{dt} = f_B = \sum_i k_{X_i B} X_i \frac{1-B}{1-B+K_{X_i A}} - \sum_i k'_{Y_i B} Y_i \frac{B}{B+K'_{Y_i B}} = 0 \quad (\text{S10})$$

where X_i (A , B , C , and/or basal) are the activating enzymes and Y_i (A , B , C , and/or basal) the deactivating enzymes. In the limiting cases where all enzymes work in either the saturated or the linear region, Eq. (S10) becomes

$$\sum_{i \in \text{saturation}} k_{X_i B} X_i + \sum_{i \in \text{linear}} k_{X_i B} X_i \frac{1-B}{K_{X_i A}} - \sum_{i \in \text{saturation}} k'_{Y_i B} Y_i - \sum_{i \in \text{linear}} k'_{Y_i B} Y_i \frac{B}{K'_{Y_i B}} = 0 \quad (\text{S11})$$

where we have split up the sums into saturating enzymes and linear enzymes. With various choices of activating/deactivating enzymes and their working limits, Eq. (S11) can establish various robust mathematical relationships among the steady state values of the nodes, A^* , B^* and C^* . For convenience, we refer to the mathematical relationships established by Eq. (S11) as the **B-algebra**. We have seen examples of the B-algebra in our discussions of adaptation mechanisms in several example networks in the main text (Eqs. (3) and (6)) and in the supplement (Eq. (S3)). The B-algebra plays a very important role for achieving robust perfect adaptation. Note that only a subset of B-algebra (and thus their corresponding B-regulation) can be used for adaptation purposes. For the NFBLB class, the B-algebra should be in the form of

$\alpha A^* + \gamma C^* + \delta = 0$, where either all three constants α , γ and δ are nonzero, or any one of them is zero. For the IFFLP class, the B-algebra should establish a proportionality relationship: $A^* \propto g(C^*)B^*$, where $g(C^*)$ is a nonzero function of C^* . We list in Figure S9 and Figure S10 all the B-regulation and the corresponding B-algebra that can be used to achieve perfect adaptation in the two classes of adaptation networks. In the following we present a general discussion on the implementation of the B-algebra in each class.

NFBLB class

As we showed in the previous section, for this class of adaptation networks $\alpha_{BB}=0$. There are only two ways to robustly achieving this: either f_B does not depend on B explicitly, i.e. $f_B = g(A,C)$ (Case 1), or the dependence on B in f_B is factorizable, i.e. $f_B = f(B) \times g(A,C)$, so that the steady state condition $g(A^*,C^*) = 0$ guarantees $\partial f_B / \partial B = 0$ at the steady state (Case 2). As can be seen from Eq. (S11), in our enzymatic model, the function $g(A,C)$ can only take linear forms in A and/or C , while $f(B)$ can only be proportional to B . For Case 1, the independence of f_B on B can be realized by not allowing any self-regulation on B and by saturating all enzymes on B -node. For Case 2, the required functional form of f_B can be realized by introducing a positive self-regulation on B that works at saturation and by letting other enzymes on B work in the linear region (an example of this case was discussed in the section “Analysis of NFBLB class with positive self-loop on B ”). In both cases, the general form of the B-algebra is $\alpha A^* + \gamma C^* + \delta = 0$. We discuss below all possible B-regulations and the corresponding B-algebra that can help achieve perfect adaptation in each of the two subsets of the NFBLB class.

(a) $\alpha_{BB}=0$ and $\beta_{AB}=0$

In this case the links $A \Rightarrow C$ and $C \Rightarrow B$ must exist while $A \Rightarrow B$ must be absent. β_{BC} can be either nonzero or zero, so the link $B \Rightarrow C$ can be either present or not. The steady state equations are $f_A(I, [A^*], [B^*], [C^*])=0$, $f_B([B^*], C^*)=0$, $f_C(A^*, [B^*], [C^*])=0$. The square brackets indicate that the variable may or may not exist depending on the network topology and the specific parameter regions the enzymes are working in. We can see that in this case f_A always contain the input I and f_C always contain the variable A , while f_B is independent of A . Thus C^* cannot be set to a constant (independent of I) by the two steady state equations $f_A=0$ and $f_C=0$. But we can set C^* to be a constant with $f_B=0$. The possible forms of f_B in this case are: $f_B(C)=\gamma C+\delta$ (only C regulates B and all MM terms are saturated) and $f_B(B, C)=B(\gamma C+\delta)$ (B activates B working at saturation and C represses B working in the linear region) -- both forms of f_B correspond to a B-algebra of the form $\gamma C^* + \delta = 0$.

(b) $\alpha_{BB}=0$ and $\beta_{BC}=0$

In this case, the links $A \Rightarrow C$ and $B \Rightarrow A$ must exist, and the link $B \Rightarrow C$ is absent. The steady state equations are $f_A(I, [A^*], B^*, [C^*])=0$, $f_B([A^*], [B^*], [C^*])=0$, $f_C(A^*, [C^*])=0$. We see that f_A always depends on the input I . Let us focus on the other two equations f_B and f_C . If f_B is independent of A i.e. no link from A to B , but dependent on C , the equation $f_B([B^*], C^*)=0$ alone can set C^* to be a constant, just like the case in (a), with or without a positive loop on B . The corresponding B-algebra is also in the form of $\gamma C^* + \delta = 0$. If f_B is dependent on A (an $A \Rightarrow B$ link), but independent on C (no $C \Rightarrow B$ link), the equation $f_B(A^*, [B^*])=0$ can set A^* to be a constant, with or without a positive self-loop on B . Since f_C depends on A and does not depend on B in this case, C^* depends solely on A^* and hence will also be a constant. The B-algebra takes the form of $\alpha A^* + \delta = 0$. If f_B is dependent both on A (an $A \Rightarrow B$ link) and on C (a $C \Rightarrow B$ link), we need two equations $f_B=0$ and

$f_C=0$ together to fix an input-independent steady state C^* . The equation $f_B(A^*,[B^*],C^*)=0$ sets up a B-algebra $\alpha A^* + \gamma C^* + \delta = 0$, which, together with $f_C(A^*,[C^*])=0$, fixes the C^* .

IFFLP class

In this category, $\beta_{AB}\beta_{BC}=\alpha_{BB}\beta_{AC}\neq 0$. In other words, we have $\frac{\partial f_B}{\partial A}\frac{\partial f_C}{\partial B}-\frac{\partial f_B}{\partial B}\frac{\partial f_C}{\partial A}=0$, but none of the derivatives in the equation can be zero. The links $A \Rightarrow B$, $A \Rightarrow C$ and $B \Rightarrow C$ must all exist. Both $f_B(A,B,[C])$ and $f_C(A,B,[C])$ must depend on A and B , and at least one of them should also depend on C . So there are three variables in the two steady state equations: $f_B(A^*,B^*,[C^*])=0$ and $f_C(A^*,B^*,[C^*])=0$. We can have a C^* that is independent of A^* and B^* only with some kind of special forms of f_B and f_C . A robust way to achieve this is (1) to have A and B regulating C with opposing signs and (2) to have B proportional to A . If $f_C(A,B,[C])=Af_1([C])-Bf_2([C])$, at steady state $A^*f_1([C^*])=B^*f_2([C^*])$. If the other steady state equation $f_B(A^*,B^*,[C^*])=0$ can establish a proportionality relationship between A^* and B^* : $A^*=g([C^*])B^*$, then C^* can be solved from these two equations and is independent of A^* and B^* . It is easy to see that f_B should take a form of $f_B = \alpha A - g(C)B$. Thus, the B-regulation in the IFFLP category of adaptation networks establishes a B-algebra of the form $A^* \propto g(C^*)B^*$, and the node B serves as a proportional node. We list in Figure S10 the regulations on B that can robustly (i.e. with the enzymes working in the two limits) generate the B-algebra of the desired form.

8. Violations of the required B-algebra compromise the network robustness

We found that although most of the adaptation networks can be classified with the listed B-regulations in Figures S9 and S10, 5 out of 166 in the NFBLB class and 33 out of 229 in the IFFLP class fall out of this classification. We closely examined each of them, and found that

none of them can achieve perfect adaptation. We found that all of them made it to the list of robust networks ($Q > 10$) by “hitchhiking” to more robust networks. That is, if a network is rather robust, then they could carry some additional “bad” (or “neutral”) links and still be reasonably robust (the resulting network could have a $Q > 10$). Consequently, we found that in all these cases, by removing the “bad” additional link(s), the network restores the “legitimate” B-regulation of perfect adaptation and its robustness increases. We also found that (not surprisingly) hitchhiking is rather common among the 395 “robust” networks, and these “bad” or “neutral” links can appear in various places in the network.

We show here one specific example in which the additional “bad” link is to the node B so that its presence confuses the classification of B-regulation. The network is shown in the upper panel of Figure S11, with the bad link colored grey. In comparison, the “true” network without the bad link is shown in the lower panel of the same figure. The kinetic equations for the hitchhiker are:

$$\begin{aligned}\frac{dA}{dt} &= Ik_{IA} \frac{(1-A)}{(1-A)+K_{IA}} - Bk'_{BA} \frac{A}{A+K'_{BA}} \\ \frac{dB}{dt} &= Ak_{AB} \frac{(1-B)}{(1-B)+K_{AB}} + Ck_{CB} \frac{(1-B)}{(1-B)+K_{CB}} - F_B k'_{F_BB} \frac{B}{B+K'_{F_BB}} \\ \frac{dC}{dt} &= Ak_{AC} \frac{(1-C)}{(1-C)+K_{AC}} - Bk'_{BC} \frac{C}{C+K'_{BC}}\end{aligned}\quad (\text{S12})$$

For a feed-forward loop, the only way to achieve perfect adaptation is for the dB/dt equation to establish a proportionality relationship between A^* and B^* . However, from Eq. (S12) we can only have $A^* k_{AB} = F_B k'_{F_BB} \frac{B^*}{K'_{F_BB}} - C^* k_{CB} \frac{(1-B^*)}{(1-B^*)+K_{CB}}$. There is no way to get rid of the C^* -dependence in this steady state equation. When we removed the grey link from C to B, the resulting network has a much higher Q (Figure S11, lower panel).

One reason for this hitchhiker network to have a relatively large Q -value (besides that the original network is even more robust) is that this additional (grey) link, though destroyed the correct B-algebra, resulted in two more negative feedback loops (compare the two networks in Figure S11). More negative feedback loops tend to have a more negative (larger absolute value) Jacobian determinant J , hence a smaller adaptation error (see Eq. (S7)). To see this, let us consider all the terms in the Jacobian determinant:

$$J = \alpha_{AA}\alpha_{BB}\alpha_{CC} + \beta_{BA}\beta_{AC}\beta_{CB} + \beta_{CA}\beta_{AB}\beta_{BC} - \alpha_{AA}\beta_{CB}\beta_{BC} - \alpha_{BB}\beta_{CA}\beta_{AC} - \alpha_{CC}\beta_{AB}\beta_{BA}.$$

Assuming no positive self-loop on any of the nodes, α_{AA} , α_{BB} , and α_{CC} are always negative. The first term is then negative. The last 5 terms in J correspond to 5 feedback loops $B \Rightarrow A \Rightarrow C \Rightarrow B$, $C \Rightarrow A \Rightarrow B \Rightarrow C$, $C \Rightarrow B \Rightarrow C$, $C \Rightarrow A \Rightarrow C$, $A \Rightarrow B \Rightarrow A$, respectively. Note that in the last three terms, the prefactors ($-\alpha_{AA}$, $-\alpha_{BB}$, and $-\alpha_{CC}$) are all positive. Thus, for all the 5 loops, a negative feedback loop would contribute to a more negative J . The more the negative feedback loops are there, the larger the absolute value of the determinant J . It is easy to see that in any 3-node networks one cannot have all 5 negative loops present simultaneously. At most there can be three negative feedback loops without creating any positive feedback loop. With four negative feedback loops there must be one positive feedback loop in coexistence (which does not help to make J more negative, because positive feedback loops decrease the absolute value of J). In this example of hitchhiker network (Figure S11), there are 3 negative feedback loops. Indeed, we found that in all the hitchhikers that messed up the B-algebra there are at least 3 negative feedback loops in each of them. These extra loops partially compensate the damage made by messing up the mechanism for perfect adaptation.

9. A special kind of coherent FFL can behavior like incoherent FFL

Note that in the IFFLP class, there are two requirements to achieve perfect adaptation: (1) the two feed-forward inputs on Node C should be *incoherent* with opposing signs, and (2) Node B serves as a proportional node (the proportionality constant can depend on C). Consider the case in which the node B is repressed by A and activated by itself, with both reactions at saturation. The steady state equation for B, $k_{BB}B^* - k'_{BB}A^* = 0$, would establish a proportional relationship between A^* and B^* . Combining this B-regulation with two more links, $A \Rightarrow C$ and $B \Rightarrow C$, of opposing signs, the resulting network would satisfy the two requirements of IFFLP adaptation class. Note that in this network the FFL is coherent, at least from a purely topological point of view. That is, the cumulative signs of the two pathways, $A \Rightarrow C$ and $A \Rightarrow B \Rightarrow C$, are the same. On the other hand, because of the special regulations on B, this coherent FFL would behave exactly like an incoherent FFL, i.e. two pathways originating from the input node exerting opposing regulations on the output node. This particular B-regulation, which leads to this counter-intuitive behavior, is not stable by itself. So this simple network with coherent FFL can not perform adaptation with the IFFLP mechanism. However, the steady state can be stabilized with the help of a negative FBL. One example of such a network is shown in Figure S12 (left panel). In this network, if the regulation on B from C is linear and others regulations on B are saturated, the steady state equation for B, $k_{BB}B^* - k'_{BB}A^* - k'_{CB}C^*B^*/K'_{CB} = 0$, also establishes a proportional relationship between A^* and B^* : $k'_{BB}A^* = (k_{BB} - k'_{CB}C^*/K'_{CB})B^*$. Thus, if the steady state is stable under some parameter sets, the network shown in Figure S12 (left panel) can in principle perform perfect adaptation with the IFFLP mechanism. We found that this network has a reasonable Q -value ($Q=11$). However, this network can also be viewed as a “hitchhiker” (see the previous section) of a more robust network of NFBLB class shown on the

right in Figure S12. The “bad” link (that decreases the Q -value) would be the negative link from A to B, which, in this case, does not mess up the B-algebra of the original NFBLB network. Indeed, we found that in about half of cases in which the network on the left in Figure S12 “adapts” (i.e. being mapped to the functional region under certain parameter set) the α_{BB} is close to zero, implying the NFBLB mechanism. For the rest of the cases, some of them seem to have adopted the IFFLP mechanism for adaptation. In any case, although it is not so robust, it is interesting to note that a coherent FFL, when dressed with a self-loop, can function like an incoherent FFL.

10. Implications of using Michaelis-Menten kinetics in our model

We used the Michaelis-Menten kinetics to model the rate equations in an enzymatic network. We examine here in detail whether certain approximations in MM kinetics will affect our conclusions. The quasi-steady-state approximation in MM kinetics assumes that the concentration of the enzyme-substrate complex is in equilibrium and does not change (or changes very slowly) with time, that is, $d[ES]/dt=0$. Since adaptation is a steady-state property, this condition is always satisfied in our analyses. Another subtlety in the MM rate equation, $k[E][S]/([S]+K)$, is that [E] is the concentration of the total enzymes while [S] is the concentration of the free (unbounded) substrate. It is often assumed that the substrate is in large excess compared with the enzyme so that [S] can be treated as the concentration of the total substrates. In an enzymatic network, an enzyme can also be a substrate and $[E_T] \ll [S_T]$ may not always hold. Furthermore, one may argue that instead of the total enzyme concentration, the circuit output should be the free enzyme concentration, which is a more relevant quantity to drive the down stream reactions. In addition, one may wonder if by introducing cooperativity in the

MM rate equations there would be different adaptation classes emerging. In the following two sections we address these issues and show that our main conclusions about the adaptation classes and their mechanisms remain unchanged.

10.1 Mass reaction equations and total Quasi-Steady-State Approximation (tQSSA)

In this section, we use the mass reaction equations to study three representative adaptation networks. In several recent papers, an approximation scheme (tQSSA) to the mass reaction equations was developed and used to model enzymatic reactions (Tzafriri 2003, Gomez-Uribe 2007, Ciliberto 2007). The method of tQSSA is considered to be applicable to a wider class of situations than the MM approximation. In tQSSA, the complexes are still assumed to reach equilibrium very fast (quasi-steady-state). But instead of using the concentration of free substrate as the dynamic variable, one focuses on the *total* substrate concentration, treating both the enzyme and the substrate on a more equal footing. In the following analyses of the adaptation networks, we first present analytic results using the tQSSA formulation to show under what conditions the network can achieve perfect adaptation. We then present numerical simulation results of the mass reaction equations to demonstrate the ability of the network to adapt.

9.1.1 NFBLB network

We use the simplest NFBLB motif (Fig. S14A, left) as an example to show in detail how tQSSA leads to the same adaptation mechanism as with the MM equations.

The mass reaction equations for this network are:

$$\begin{aligned}
\frac{d[IA]}{dt} &= k_{IA1}[I][A] - (k_{IA-1} + k_{IA2})[IA] \\
\frac{d[B_P A_P]}{dt} &= k_{B_P A_P 1}[B_P][A_P] - (k_{B_P A_P -1} + k_{B_P A_P 2})[B_P A_P] \\
\frac{d[A_P B]}{dt} &= k_{A_P B 1}[A_P][B] - (k_{A_P B -1} + k_{A_P B 2})[A_P B] \\
\frac{d[E_0 B_P]}{dt} &= k_{E_0 B_P 1}[E_0][B_P] - (k_{E_0 B_P -1} + k_{E_0 B_P 2})[E_0 B_P] \\
\frac{d[A_{PT}]}{dt} &= k_{IA2}[IA] - k_{B_P A_P 2}[B_P A_P] \\
\frac{d[B_{PT}]}{dt} &= k_{A_P B 2}[A_P B] - k_{E_0 B_P 2}[E_0 B_P] \\
[A_{PT}] &= [A_P] + [B_P A_P] + [A_P B] \\
[B_{PT}] &= [B_P] + [E_0 B_P] + [B_P A_P]
\end{aligned} \tag{S13}$$

where A_p (B_p) and A (B) denote the active and the inactive form of the node A (B), respectively.

With the assumption of quasi steady state for the complexes, and the assumption that the square of the complex concentration is much smaller than the product of the free enzyme and the free substrate concentrations ($[ES]^2 \ll [E][S]$ for all the reactions), we get:

$$\begin{aligned}
k_{IA1}[I][A] - (k_{IA-1} + k_{IA2})[IA] &= 0 \\
k_{B_P A_P 1}[B_P][A_P] - (k_{B_P A_P -1} + k_{B_P A_P 2})[B_P A_P] &= 0 \\
k_{A_P B 1}[A_P][B] - (k_{A_P B -1} + k_{A_P B 2})[A_P B] &= 0 \\
k_{E_0 B_P 1}[E_0][B_P] - (k_{E_0 B_P -1} + k_{E_0 B_P 2})[E_0 B_P] &= 0 \\
\frac{d[A_{PT}]}{dt} &= k_{IA2}[IA] - k_{B_P A_P 2}[B_P A_P] \\
&= k_{IA2} \frac{[I_T]([A] + [IA])}{K_{IA} + [I_T] + [A] + [IA]} - k_{B_P A_P 2} \frac{([B_P] + [B_P A_P])([A_P] + [B_P A_P])}{K_{B_P A_P} + [B_P] + [B_P A_P] + [A_P] + [B_P A_P]} \\
\frac{d[B_{PT}]}{dt} &= k_{A_P B 2}[A_P B] - k_{E_0 B_P 2}[E_0 B_P] \\
&= k_{A_P B 2} \frac{([A_P] + [A_P B])([B] + [A_P B])}{K_{A_P B} + [A_P] + [A_P B] + [B] + [A_P B]} - k_{E_0 B_P 2} \frac{[E_{0T}](B_P) + [E_0 B_P]}{K_{E_0 B_P} + [E_{0T}] + [B_P] + [E_0 B_P]} \tag{S14}
\end{aligned}$$

We can see that the difference between the new rate equations (Eq. S14) and the Michaelis-Menten equations is that in Eq. (S14) the enzymatic reaction terms have the form

$[E'][S']/(K_m+[E']+[S'])$, where $[E']$ and $[S']$ are the total enzyme and the total substrate that is involved in the particular reaction, respectively. Thus, the competition between different substrates and/or different enzymes is included in this formulism. Also note that $[E_T] \ll [S_T]$ is no longer an implicit assumption for the new equations.

In the model of the Michaelis-Menten equations, the condition to have perfect adaptation is to saturate the two reactions on the node B. Similarly, in this model, the condition for the total enzyme concentration $[A_p]+[A_pB]$ to be a constant is to saturate the two reactions:

$$\begin{aligned} [B]+[A_pB] &>> K_{A_pB} \quad \text{and} \quad [B]+[A_pB] >> [A_p]+[A_pB] \\ [B_p]+[E_0B_p] &>> K_{E_0B_p} \quad \text{and} \quad [B_p]+[E_0B_p] >> E_{0T} \end{aligned} \quad (\text{S15})$$

We found that it is still necessary to have a larger total substrate concentration than the total enzyme concentration. But this constraint is only for the two key regulations on the node B. By applying the condition of Eq. (S15), we have:

$$\frac{d[B_{PT}]}{dt} = k_{A_pB2}([A_p]+[A_pB]) - k_{E_0B_p2}[E_{0T}] \quad (\text{S16})$$

which implies a constant steady state for $[A_p]+[A_pB]$. Therefore, as far as the total enzyme concentration is concerned, the adaptation mechanism and condition is the same as for the MM equations.

10.1.2 Adaptation in the free form of the enzyme

If one wants to use the free form $[A_p]$ as the output and require it to be a constant, we should satisfy the condition that $[A_p]$ and $[A_p]+[A_pB]$ are similar, or $[A_p] \gg [A_pB]$, which would then imply $[A_p] \approx [A_p]+[A_pB] = \text{constant}$. In other words, the measurement of the output A_p made by the buffer node B should not disturb the output itself significantly. With the network topology

shown on the left of Fig S14A, the output node A directly acts on the buffer node B. For the free form $[A_P]$, we have the following formulae:

$$\frac{[A_P]}{[A_P B]} = \frac{K_{A_P B}}{[B]} \quad (\text{S17})$$

Since perfect adaptation requires this reaction to be saturated, normally we have $[B] \gg K_{A_P B}$, implying $[A_P B] \gg [A_P]$. This means that most of the active form A_P is bound with B, leaving only very few free A_P for other reactions (e.g. serving as the output signal). If we want to have more free form in the output, an additional intermediate node between A and B can be introduced, which we denote as node D (Fig. S14A, right). The node D here serves as an information relay of the output signal but with a minimal disturbance to the output itself, which can be achieved by a low concentration of D compared with A_P or by making the reaction from A to D linear. The perfect adaption condition is still on the node B, i.e. the reactions from D to B and from the basal enzyme E_0 to B are saturated. Mathematically, with the additional node D, the mass reaction equations with the tQSSA are:

$$\begin{aligned} k_{IA1}[I][A] - (k_{IA-1} + k_{IA2})[IA] &= 0 \\ k_{B_P A_P 1}[B_P][A_P] - (k_{B_P A_P -1} + k_{B_P A_P 2})[B_P A_P] &= 0 \\ k_{D_P B 1}[D_P][B] - (k_{D_P B -1} + k_{D_P B 2})[D_P B] &= 0 \\ k_{E_0 B_P 1}[E_0][B_P] - (k_{E_0 B_P -1} + k_{E_0 B_P 2})[E_0 B_P] &= 0 \\ k_{A_P D 1}[A_P][D] - (k_{A_P D -1} + k_{A_P D 2})[A_P D] &= 0 \\ k_{E_1 D_P 1}[E_1][D_P] - (k_{E_1 D_P -1} + k_{E_1 D_P 2})[E_1 D_P] &= 0 \\ k_{E_1 D_P 1}[E_1][D_P B] - (k_{E_1 D_P -1} + k_{E_1 D_P 2})[E_1 D_P B] &= 0 \\ k_{D_P B 1}[E_1 D_P][B] - (k_{D_P B -1} + k_{D_P B 2})[E_1 D_P B] &= 0 \\ [A_{PT}] &= [A_P] + [B_P A_P] + [A_P D] \\ [B_{PT}] &= [B_P] + [E_0 B_P] + [B_P A_P] \\ [D_{PT}] &= [D_P] + [E_1 D_P] + [D_P B] + [E_1 D_P B] \end{aligned}$$

$$\begin{aligned}
\frac{d[A_{PT}]}{dt} &= k_{IA2}[IA] - k_{B_pA_p2}[B_pA_p] \\
&= k_{IA2} \frac{[I_T]([A] + [IA])}{K_{IA} + [I_T] + [A] + [IA]} - k_{B_pA_p2} \frac{([B_p] + [B_pA_p])([A_p] + [B_pA_p])}{K_{B_pA_p} + [B_p] + [B_pA_p] + [A_p] + [B_pA_p]} \\
\frac{d[B_{PT}]}{dt} &= k_{D_pB2}([D_pB] + [E_1D_pB]) - k_{E_0B_p2}[E_0B_p] \\
&= k_{D_pB2} \frac{([D_p] + [D_pB] + [E_1D_p] + [E_1D_pB])([B] + [D_pB] + [E_1D_pB])}{K_{D_pB} + [D_p] + [D_pB] + [E_1D_p] + [E_1D_pB] + [B] + [D_pB] + [E_1D_pB]} \\
&\quad - k_{E_0B_p2} \frac{[E_{0T}]([B_p] + [E_0B_p])}{K_{E_0B_p} + [E_{0T}] + [B_p] + [E_0B_p]} \\
&= k_{D_pB2} \frac{[D_{PT}]([B_T] - [B_{PT}])}{K_{D_pB} + [D_{PT}] + [B_T] - [B_{PT}]} - k_{E_0B_p2} \frac{[E_{0T}]([B_p] + [E_0B_p])}{K_{E_0B_p} + [E_{0T}] + [B_p] + [E_0B_p]} \tag{S18} \\
\frac{d[D_{PT}]}{dt} &= k_{A_pD2}[A_pD] - k_{E_1D_p2}([E_1D_p] + [E_1D_pB]) \\
&= k_{A_pD2} \frac{([A_p] + [A_pD])([D] + [A_pD])}{K_{A_pD} + [A_p] + [A_pD] + [D] + [A_pD]} \\
&\quad - k_{E_1D_p2} \frac{[E_{1T}]([D_p] + [E_1D_p] + [D_pB] + [E_1D_pB])}{K_{E_1D_p} + [E_{1T}] + [D_p] + [E_1D_p] + [D_pB] + [E_1D_pB]} \\
&= k_{A_pD2} \frac{([A_p] + [A_pD])([D_T] - [D_{PT}])}{K_{A_pD} + [A_p] + [A_pD] + [D_T] - [D_{PT}]} - k_{E_1D_p2} \frac{[E_{1T}][D_{PT}]}{K_{E_1D_p} + [E_{1T}] + [D_{PT}]}
\end{aligned}$$

where we assumed that E_1 works on both free D_p and the complex form D_pB . Saturating the two reactions on the node B (see the $d[B_{PT}]/dt$ equation) gives $[D_{PT}] = \text{constant}$. From the equation $d[D_{PT}]/dt = 0$, we see that $[A_p] + [A_pD]$ is a function of $[D_{PT}]$, implying that $[A_p] + [A_pD]$ will also be a constant when $[D_{PT}] = \text{constant}$. Then, with $[A_p] \gg [A_pD]$ (by either making $[D_T] \ll [A_T]$ or making the A to D reaction linear), we can approach perfect adaptation in the free form concentration $[A_p]$ of the enzyme.

10.1.3 Simulation of the full mass reaction equations

In Fig. S13A (lower panels) we show the simulation results of a full set of mass reaction kinetic equations (no quasi-steady-state approximations), in comparison with the numerical simulations of MM equations.

The IFFLP motif

Using the tQSSA, for the IFFLP adaptation network (Fig. S13B, left) we have the following equations for node B and node C:

$$\begin{aligned} \frac{d[B_{PT}]}{dt} &= k_{A_p B^2} \frac{([A_p] + [A_p B])([B] + [A_p B])}{K_{A_p B} + [A_p] + [A_p B] + [B] + [A_p B]} \\ &\quad - k_{E_0 B_p}^2 \frac{E_{0T}([B_p] + [E_0 B_p])}{K_{E_0 B_p} + E_{0T} + [B_p] + [E_0 B_p]} \\ \frac{d[C_{PT}]}{dt} &= k_{A_p C^2} \frac{([A_p] + [A_p C])([C] + [A_p C])}{K_{A_p C} + [A_p] + [A_p C] + [C] + [A_p C]} \\ &\quad - k_{B_p C_p}^2 \frac{([B_p] + [B_p C_p])([C_p] + [B_p C_p])}{K_{B_p C_p} + [B_p] + [B_p C_p] + [C_p] + [B_p C_p]} \end{aligned} \quad (\text{S19})$$

Suppose the first term in $d[B_{PT}]/dt$ equation is saturated and the second linear, we have:

$$\begin{aligned} \frac{d[B_{PT}]}{dt} &= k_{A_p B^2}([A_p] + [A_p B]) - k_{E_0 B_p}^2 \frac{E_{0T}([B_p] + [E_0 B_p])}{K_{E_0 B_p} + E_{0T}} \\ \frac{d[C_{PT}]}{dt} &= k_{A_p C^2} \frac{([A_p] + [A_p C])([C] + [A_p C])}{K_{A_p C} + ([A_p] + [A_p C]) + ([C] + [A_p C])} \\ &\quad - k_{B_p C_p}^2 \frac{([B_p] + [B_p C_p])([C_p] + [B_p C_p])}{K_{B_p C_p} + ([B_p] + [B_p C_p]) + ([C_p] + [B_p C_p])} \end{aligned} \quad (\text{S20})$$

In the Michaelis-Menten formulation, the steady-state condition for the two equations will guarantee perfect adaptation. However, here the proportional relationship, $[A_p] + [A_p B] \propto [B_p] + [E_0 B_p]$, established by $d[B_{PT}]/dt = 0$ equation does not always lead to the elimination of A_p and B_p in the $d[C_{PT}]/dt = 0$ equation, a condition required for perfect adaptation. We see that to achieve robust perfect adaptation in Eq. (S20) we should have (1) the concentration of the free form (enzymes and substrates) much larger than that of the complex forms, and (2) the substrate concentration much larger than its enzyme concentration in both terms of the $d[C_{PT}]/dt$ equation. The condition (2) is the implicit assumption in MM equations. For condition (1), it can be easily

achieved for all enzymes and substrates by either adjust their relative concentrations or making the enzyme working in the linear region, except for the reaction $A_P \rightarrow B$ which must work in the saturated region due to the perfect adaptation constraint implying $[A_P B] > [A_P]$. This problem can be resolved by introducing an additional node D between A and B as indicated in Fig. S14B, where E_1 works on both the free form $[D_P]$ and the complex form $[D_P B]$. The network can achieve adaptation with the same mechanism as found with MM equations.

10.1.4 NFBLB with positive self loop

For the NFBLB network with an auto-positive feedback loop on B (Fig. S13C), the tQSSA gives the following equation for node B:

$$\frac{d[B_{PT}]}{dt} = k_{B_P B^2} \frac{([B_P] + [A_P B_P] + [B_P B] + [A_P B_P B])([B] + [B_P B] + [A_P B_P B])}{K_{B_P B} + [B_P] + [A_P B_P] + [B_P B] + [A_P B_P B] + [B] + [B_P B] + [A_P B_P B]} - k_{A_P B_P^2} \frac{([A_P] + [A_P B_P] + [A_P B_P B])([B_P] + [A_P B_P] + [B_P B] + [A_P B_P B])}{K_{A_P B_P} + [A_P] + [A_P B_P] + [A_P B_P B] + [B_P] + [A_P B_P] + [B_P B] + [A_P B_P B]} \quad (\text{S21})$$

where we assumed that A_P works on both the free form B_P and the complex form $B_P B$. If the first term in Eq. (S21) is in the saturated region and the second one in the linear region, we have:

$$\frac{d[B_{PT}]}{dt} = [B_{PT}] (k_{B_P B^2} - k_{A_P B_P^2} \frac{[A_P] + [A_P B_P] + [A_P B_P B]}{K_{A_P B_P} + [A_P] + [A_P B_P] + [A_P B_P B]}) \quad (\text{S22})$$

Thus, the total enzyme $[A_{pT}]$ adapts with the same mechanism found with the MM equations. If one requires the free enzyme $[A_p]$ to adapt, it can be easily achieved in this case since $A_P - |B_P$ works in the linear region, the complex concentration can easily be much less than the free form, giving $[A_P] \approx [A_P] + [A_P B_P] + [A_P B_P B] = [A_{pT}]$.

10.2 Cooperative regulations

We have also studies all of the 3-node enzymatic circuits with cooperative regulations.

Specifically, we replaced the usual MM kinetics $E \frac{S}{S + K}$ with $E \frac{S^n}{S^n + K^n}$ in all equations, and let the Hill coefficient n to be a variable of the range 1 to 4. Note that just like the other parameters k_{cat} and K_M , n can be different for different reactions in the circuit. We sampled 10,000 parameter sets for each network topology. In general, there is a decrease in robustness (\mathcal{Q}), presumably due to the increased number of circuit parameters.

Our results can be summarized as follows. (1) There are no new classes of adaptation compared with the simple MM kinetics. (2) The NFBLB without the auto-positive loop is the most robust class of adaptation. The most robust topologies are those with multiple negative feedback loops. This is because that for this class of topologies the adaptation is achieved via the saturation of enzymes by substrates at the key node (B). Higher Hill coefficients can help to achieve the saturation condition $(S / K)^n \gg 1$. However, higher Hill coefficients do not result in any new adaptation mechanism. In particular, it is still necessary to have a buffer node (B) acting as an integrator in this class. (3) The IFFLP class is less robust. This is because that one condition for adaptation in this class requires a linear dependence of the rate on the substrate concentration in order for the node B to be a proportioner. This linear dependence can only be achieved with Hill coefficient $n=1$. This fact can be easily seen from the equation for Node B

$$\text{(compare with Eq. (5) in the main text): } \frac{dB}{dt} = Ak_{AB} \frac{(1-B)^{n_{AB}}}{(1-B)^{n_{AB}} + K_{AB}^{n_{AB}}} - F_B k'_{F_B B} \frac{B^{n_{F_B B}}}{B^{n_{F_B B}} + K'_{F_B B}^{n_{F_B B}}}. A$$

proportional relationship between Node A and Node B can only be established when $n_{F_B B} = 1$ (and with the first term saturated and the second in the linear region). Thus, in this case any Hill

coefficients higher than 1 would hinder the adaptation. This could be a potential reason why the IFFLP topologies seem to appear much less often in natural adaptation circuits. (4) For a similar reason, the topologies in NFBLB class with an auto-positive loop on Node B are less robust. There we also need a linear dependence of rate on substrate which can only be realized with $n=1$. The equation for Node B is (compare with Eq. (S2)):

$$\frac{dB}{dt} = B k_{BB} \frac{(1-B)^{n_{BB}}}{(1-B)^{n_{BB}} + K_{BB}^{n_{BB}}} - C k'_{CB} \frac{B^{n_{CB}}}{B^{n_{CB}} + K'^{n_{CB}}_{CB}}. \text{ Perfect adaptation is possible only if } n_{CB} = 1,$$

so that the B dependence in the first term cancels out that on the second term when the first term is saturated and the second in the linear region.

11. Effects of different sampling sizes and of precision and sensitivity thresholds

Our numerical results presented in the main text were obtained by sampling 10,000 sets of parameters for each network architecture. To test whether our main conclusions depend on sampling size we sampled 1,000 sets of parameters for each network. The Q-values from the 10,000 samples and the 1,000 samples are highly correlated (correlation coefficient 0.86) (Fig. S14A). We found that sampling with only 1,000 sets of parameters can identify the most robust networks, but will miss some of the simplest NFBLB motifs. With 10,000 samples, most of the adaptation networks are identified, from which we can extract the design rules governing all of them.

In the main text, we define a circuit to be functional if its sensitivity > 1 and precision > 10 . If we change the sensitivity cutoff to 0.5 and the precision cutoff to 5 (i.e. the circuit is functional if sensitivity > 0.5 and precision > 5), we get 1341 networks each of which has more than 10 sets of functional parameters (with 10,000 sampling size). The correlation coefficient between this

data set and the previous data set is 0.94 (Fig. S14B). More importantly, all the 1341 networks contain at least one negative feedback loop or one incoherent feed-forward loop.

12. Design table for adaptation networks

The discussion about the relationship of the feedback loops with the Jacobian determinant, presented in the last paragraph of the section “Violations of the required B-algebra compromise the network robustness”, provides an explanation for our numerical observation that certain additional negative feedback loops can improve the network’s robustness. We found that the improvements are most obvious if these additional negative loops go through the control node B in ways that do not contradict any adaptation mechanism. Note that the negative feedback loop between the nodes A and C (which does not go through the node B), does not contribute to the Jacobian determinant J in the two adaptation classes. This loop appears in J together with the diagonal element $\alpha_{BB}=0$ as a product term, $\alpha_{BB}\beta_{AC}\beta_{CA}$ (Eq. (S9)). For the NFBLB class, we always have $\alpha_{BB}=0$ so that this term is always zero. For the IFFLP class, $\alpha_{BB}\beta_{AC}=\beta_{AB}\beta_{BC}$ which implies $\alpha_{BB}\beta_{AC}\beta_{CA}=\beta_{AB}\beta_{BC}\beta_{CA}$, so that this term cancels out another term in J : $\beta_{AB}\beta_{BC}\beta_{CA}-\alpha_{BB}\beta_{AC}\beta_{CA}=0$ (see Eq. (S9)). This means that in IFFLP class, creating a feedback loop $A \Rightarrow C \Rightarrow A$ (positive or negative) would always simultaneously create a feedback loop $A \Rightarrow B \Rightarrow C \Rightarrow A$ which exactly cancels out any effects of the $A \Rightarrow C \Rightarrow A$ loop on the determinant J .

In Figure S15, we provide a full design table of adaptation networks, constructed by adding to the core adaptation topologies more and more negative feedback loops that (1) go through the node B, (2) do not violate the adaptation mechanism (the B-algebra), and (3) do not result in any positive feedback loops. We see that for most cases additions of these loops increased the robustness (green arrows). For the few cases in which the robustness is decreased (red arrows),

the additional loops increased the number of network parameters, which may result in a drop of Q -value. When the number of network parameters is increased, the dimensions of parameter space increase. This tends to decrease the Q -value. An intuitive explanation for this is that if each parameter has 50% chance of being functional, the total fraction of functional parameter sets for a network with n parameters is then 0.5^n , which decreases quickly with n . Note that even some additional loops increased the number of parameters (e.g. the network (I) or (II) being changed to network (IV) in Figure S15), the robustness still increased.

We provide below a detailed analysis for some example networks. These networks are marked with a number next to it in Figure S15.

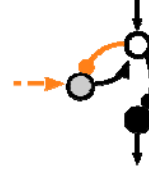
See Figure S14 for the full design table

(I) **Key topological features:** Single negative feedback loop. Node B is regulated only by A. Output node C is only regulated by A, hence $A^*=\text{constant}$ implies $C^*=\text{constant}$.

Parameter constraints: The two reactions acting on Node B are saturated.

The equations are:

$$\begin{aligned}\frac{dA}{dt} &= I k_{IA} \frac{(1-A)}{(1-A)+K_{IA}} + B k_{BA} \frac{(1-A)}{(1-A)+K_{BA}} - F_A k'_{F_AA} \frac{A}{A+K'_{F_AA}} \\ \frac{dB}{dt} &= E_B k_{E_BB} \frac{(1-B)}{(1-B)+K_{E_BB}} - A k'_{AB} \frac{B}{B+K'_{AB}} \\ \frac{dC}{dt} &= E_C k_{E_CC} \frac{(1-C)}{(1-C)+K_{E_CC}} - A k'_{AC} \frac{C}{C+K'_{AC}}\end{aligned}$$



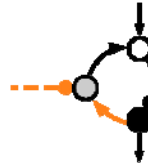
If the two reactions on Node B are saturated, $A = E_B k_{E_BB} / k'_{AB}$. From the third equation we see that the steady state level of C is only dependent on the concentration of A. So at steady state C^* is also a constant independent of the input.

(II) **Key topological features:** Single negative feedback loop. Node B is regulated only by the output node C.

Parameter constraints: The two reactions acting on B are saturated.

The equations are:

$$\begin{aligned}\frac{dA}{dt} &= I k_{IA} \frac{(1-A)}{(1-A)+K_{IA}} + B k_{BA} \frac{(1-A)}{(1-A)+K_{BA}} - F_A k'_{F_AA} \frac{A}{A+K'_{F_AA}} \\ \frac{dB}{dt} &= C k_{CB} \frac{(1-B)}{(1-B)+K_{CB}} - F_B k'_{F_BB} \frac{B}{B+K'_{F_BB}} \\ \frac{dC}{dt} &= E_C k_{E_CC} \frac{(1-C)}{(1-C)+K_{E_CC}} - A k'_{AC} \frac{C}{C+K'_{AC}}\end{aligned}$$



If the two reactions on B are saturated, $C = F_B k'_{F_BB} / k_{CB}$.

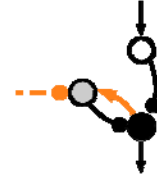
See Figure S14 for the full design table

(III) **Key topological features:** Single negative feedback loop. Node B is regulated only by the output node C.

Parameter constraints: The two reactions acting on B are saturated.

The equations are:

$$\begin{aligned}\frac{dA}{dt} &= Ik_{IA} \frac{(1-A)}{(1-A)+K_{IA}} - F_A k'_{F_A A} \frac{A}{A+K'_{F_A A}} \\ \frac{dB}{dt} &= Ck_{CB} \frac{(1-B)}{(1-B)+K_{CB}} - F_B k'_{F_B B} \frac{B}{B+K'_{F_B B}} \\ \frac{dC}{dt} &= Ak_{AC} \frac{(1-C)}{(1-C)+K_{AC}} - Bk'_{BC} \frac{C}{C+K'_{BC}}\end{aligned}$$



If the two reactions on B are saturated, $C^* = F_B k'_{F_B B} / k_{CB} = \text{constant}$.

(IV) **Key topological features:** Two negative feedback loops. Node B is regulated by both A and C.

Parameter constraints: The two reactions acting on B are saturated.

The equations are:

$$\begin{aligned}\frac{dA}{dt} &= Ik_{IA} \frac{(1-A)}{(1-A)+K_{IA}} + Bk_{BA} \frac{(1-A)}{(1-A)+K_{BA}} - F_A k'_{F_A A} \frac{A}{A+K'_{F_A A}} \\ \frac{dB}{dt} &= Ck_{CB} \frac{(1-B)}{(1-B)+K_{CB}} - Ak'_{AB} \frac{B}{B+K'_{AB}} \\ \frac{dC}{dt} &= E_C k_{E_C C} \frac{(1-C)}{(1-C)+K_{E_C C}} - Ak'_{AC} \frac{C}{C+K'_{AC}}\end{aligned}$$



If the two reactions on B are saturated, $A * k'_{AB} = C * k_{CB}$. Together with the steady state equation for C, we

have

$$\left\{ \begin{array}{l} A * k'_{AB} - C * k_{CB} = 0 \\ E_C k_{E_C C} \frac{(1-C^*)}{(1-C^*)+K_{E_C C}} - Ak'_{AC} \frac{C^*}{C^*+K'_{AC}} = 0 \end{array} \right.$$

These two equations give unique solutions of A^* and C^* , independent of the input.

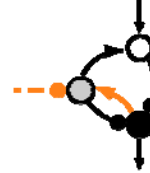
See Figure S14 for the full design table

(V) **Key topological features:** Two negative feedback loops. Node B is regulated by C, but feeds back to both Node A and Node C.

Parameter constraints: The two regulations acting on B are saturated.

The equations are:

$$\begin{aligned}\frac{dA}{dt} &= I k_{IA} \frac{(1-A)}{(1-A)+K_{IA}} - B k'_{BA} \frac{A}{A+K'_{BA}} \\ \frac{dB}{dt} &= C k_{CB} \frac{(1-B)}{(1-B)+K_{CB}} - F_B k'_{F_B B} \frac{B}{B+K'_{F_B B}} \\ \frac{dC}{dt} &= A k_{AC} \frac{(1-C)}{(1-C)+K_{AC}} - B k'_{BC} \frac{C}{C+K'_{BC}}\end{aligned}$$



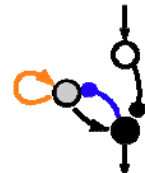
If the two reactions on B are saturated, $C^* = F_B k'_{F_B B} / k_{CB} = \text{constant}$.

(VI) **Key topological features:** Single negative feedback loop plus a positive self-loop on B. Apart from the B self-regulation, the other regulations to B must be negative.

Parameter constraints: The B self-regulation is saturated. The other regulation on B is linear.

The equations are:

$$\begin{aligned}\frac{dA}{dt} &= I k_{IA} \frac{(1-A)}{(1-A)+K_{IA}} - F_A k'_{F_A A} \frac{A}{A+K'_{F_A A}} \\ \frac{dB}{dt} &= B k_{BB} \frac{(1-B)}{(1-B)+K_{BB}} - C k'_{CB} \frac{B}{B+K'_{CB}} \\ \frac{dC}{dt} &= B k_{BC} \frac{(1-C)}{(1-C)+K_{BC}} - A k'_{AC} \frac{C}{C+K'_{AC}}\end{aligned}$$



If the first reaction on Node B is in the linear region and the second saturated, $B^*(k_{BB} - C^* k'_{CB} / K'_{CB}) = 0$. B^*

is not 0, $C^* = k_{BB} K'_{CB} / k'_{CB} = \text{constant}$.

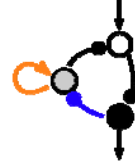
See Figure S14 for the full design table

(VII) **Key topological features:** Single negative feedback loop plus a positive self-loop on B. Apart from the B self-regulation, the other regulations to B must be negative.

Parameter constraints: The B self-regulation is saturated. The other regulation on B is linear.

The equations are:

$$\begin{aligned}\frac{dA}{dt} &= Ik_{IA} \frac{(1-A)}{(1-A)+K_{IA}} - Bk'_{BA} \frac{A}{A+K'_{BA}} \\ \frac{dB}{dt} &= Bk_{BB} \frac{(1-B)}{(1-B)+K_{BB}} - Ck'_{CB} \frac{B}{B+K'_{CB}} \\ \frac{dC}{dt} &= E_C k_{EcC} \frac{(1-C)}{(1-C)+K_{EcC}} - Ak'_{AC} \frac{C}{C+K'_{AC}}\end{aligned}$$



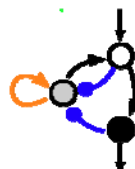
If the first reaction on node B is linear and the second reaction saturated, $B^* (\mathbb{k}^{BB} - C^* \mathbb{k}_{CB}^{CB} / K_{CB}^{CB}) = 0 \cdot B^*$ is not 0, $C^* = k_{BB} K_{CB}^{CB} / k'_{CB} = \text{constant}$.

(VIII) **Key topological features:** Two negative feedback loops plus a positive self-loop on B. Apart from the B self-regulation, the other regulations on B must be negative.

Parameter constraints: The B self-regulation is saturated. The other regulations on B are linear.

The equations are:

$$\begin{aligned}\frac{dA}{dt} &= Ik_{IA} \frac{(1-A)}{(1-A)+K_{IA}} + Bk_{BA} \frac{(1-A)}{(1-A)+K_{BA}} - F_A k'_{F_AA} \frac{A}{A+K'_{F_AA}} \\ \frac{dB}{dt} &= Bk_{BB} \frac{(1-B)}{(1-B)+K_{BB}} - Ak'_{AB} \frac{B}{B+K'_{AB}} - Ck'_{CB} \frac{B}{B+K'_{CB}} \\ \frac{dC}{dt} &= Ak_{AC} \frac{(1-C)}{(1-C)+K_{AC}} - F_C k'_{F_CC} \frac{C}{C+K'_{F_CC}}\end{aligned}$$



If the first reaction on node B is linear, and the second and the third reactions are saturated, $B^* (k_{BB} - A^* k'_{AB} / K'_{AB} - C^* k'_{CB} / K'_{CB}) = 0 \cdot B^*$ is not 0. C^* can be fixed together with the steady state equation for dC/dt :

$$\left\{ \begin{array}{l} k_{BB} - A^* k'_{AB} / K'_{AB} - C^* k'_{CB} / K'_{CB} = 0 \\ A^* k_{AC} \frac{(1-C^*)}{(1-C^*)+K_{AC}} - F_C k'_{F_CC} \frac{C^*}{C^*+K'_{F_CC}} \end{array} \right.$$

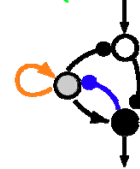
See Figure S14 for the full design table

(IX) **Key topological feature:** Two negative feedback loops plus a positive self-loop on B. Apart from the B self-regulation, the other regulations on B must be negative.

Parameter constraints: The B self-regulation is saturated. The other regulation on B is linear.

The equations are:

$$\begin{aligned}\frac{dA}{dt} &= Ik_{IA} \frac{(1-A)}{(1-A)+K_{IA}} - Bk'_{BA} \frac{A}{A+K'_{BA}} \\ \frac{dB}{dt} &= Bk_{BB} \frac{(1-B)}{(1-B)+K_{BB}} - Ck'_{CB} \frac{B}{B+K'_{CB}} \\ \frac{dC}{dt} &= Bk_{BC} \frac{(1-C)}{(1-C)+K_{BC}} - Ak'_{AC} \frac{C}{C+K'_{AC}}\end{aligned}$$



If the first reaction on Node B is linear and the second saturated, $B^*(k_{BB} - C^* k'_{CB} / K'_{CB}) = 0$. B^* is not 0,

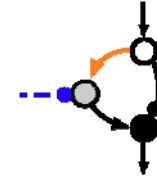
$$C^* = k_{BB} K'_{CB} / k'_{CB} = \text{constant}.$$

(X) **Key topological features:** Incoherent feed-forward loop. The regulation from A to C has a different sign as the regulation from B to C. The regulation from A to B is positive.

Parameter constraints: The regulation from A to B is saturated. The basal regulation on B is linear.

The equations are:

$$\begin{aligned}\frac{dA}{dt} &= Ik_{IA} \frac{(1-A)}{(1-A)+K_{IA}} - F_A k'_{F_AA} \frac{A}{A+K'_{F_AA}} \\ \frac{dB}{dt} &= Ak_{AB} \frac{(1-B)}{(1-B)+K_{AB}} - F_B k'_{F_BB} \frac{B}{B+K'_{F_BB}} \\ \frac{dC}{dt} &= Bk_{BC} \frac{(1-C)}{(1-C)+K_{BC}} - Ak'_{AC} \frac{C}{C+K'_{AC}}\end{aligned}$$



If the first (activation) reaction on Node B is saturated and the other linear, $A^* = B^* F_B k'_{F_BB} / k_{AB} / K'_{F_BB}$.

Substituting it into the third equation at steady state, we have

$$k_{BC} \frac{(1-C^*)}{(1-C^*)+K_{BC}} - \frac{F_B k'_{F_BB}}{k_{AB} K'_{F_BB}} k'_{AC} \frac{C^*}{C^*+K'_{AC}} = 0$$

C^* is a constant independent of the input.

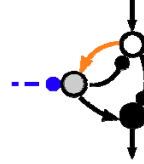
See Figure S14 for the full design table

(XI) **Key topological features:** Incoherent feed-forward loop coupled with one negative feedback loop. The regulation from A to C has a different sign as the regulation from B to C. The regulation from A to B is positive.

Parameter constraints: The regulation from A to B is saturated. The other regulation on B is linear.

The equations are:

$$\begin{aligned}\frac{dA}{dt} &= Ik_{IA} \frac{(1-A)}{(1-A)+K_{IA}} - Bk'_{BA} \frac{A}{A+K'_{BA}} \\ \frac{dB}{dt} &= Ak_{AB} \frac{(1-B)}{(1-B)+K_{AB}} - F_B k'_{F_BB} \frac{B}{B+K'_{F_BB}} \\ \frac{dC}{dt} &= Bk_{BC} \frac{(1-C)}{(1-C)+K_{BC}} - Ak'_{AC} \frac{C}{C+K'_{AC}}\end{aligned}$$



If the first (activation) reaction on B is saturated and the other linear, $A^* = B^* F_B k'_{F_BB} / k_{AB} / K'_{F_BB}$. Substituting it into the third equation at steady state, we have

$$k_{BC} \frac{(1-C^*)}{(1-C^*)+K_{BC}} - \frac{F_B k'_{F_BB}}{k_{AB} K'_{F_BB}} k'_{AC} \frac{C^*}{C^*+K'_{AC}} = 0 \quad \text{where } C^* \text{ is a constant independent of the input.}$$

(XII) **Key topological features:** Incoherent feed-forward loop coupled with one negative feedback loop. The regulation from A to C has a different sign as the regulation from B to C. The regulation from A to B is positive.

Parameter constraints: The regulation from A to B is saturated. The other regulation on B is linear.

The equations are:

$$\begin{aligned}\frac{dA}{dt} &= Ik_{IA} \frac{(1-A)}{(1-A)+K_{IA}} - F_A k'_{F_AA} \frac{A}{A+K'_{F_AA}} \\ \frac{dB}{dt} &= Ak_{AB} \frac{(1-B)}{(1-B)+K_{AB}} - Ck'_{CB} \frac{B}{B+K'_{CB}} \\ \frac{dC}{dt} &= Bk_{BC} \frac{(1-C)}{(1-C)+K_{BC}} - Ak'_{AC} \frac{C}{C+K'_{AC}}\end{aligned}$$



If the first (activation) reaction on B is saturated and the other linear, $A^* = B^* C^* k'_{CB} / k_{AB} / K'_{CB}$. Substituting it into the third equation at steady state, we have

$$k_{BC} \frac{(1-C^*)}{(1-C^*)+K_{BC}} - \frac{C^* k'_{CB}}{k_{AB} K'_{CB}} k'_{AC} \frac{C^*}{C^*+K'_{AC}} = 0 \quad \text{where } C^* \text{ is a constant independent of input.}$$

See Figure S14 for the full design table

(XIII) **Key topological features:** Incoherent feed-forward loop coupled with three negative feedback loops.

The regulation from A to C has a different sign as the regulation from B to C. The regulation from A to B is positive.

Parameter constraints: The regulation from A to B is saturated. The other regulation on B is linear.

The equations are:

$$\begin{aligned}\frac{dA}{dt} &= Ik_{IA} \frac{(1-A)}{(1-A)+K_{IA}} - Bk'_{BA} \frac{A}{A+K'_{BA}} \\ \frac{dB}{dt} &= Ak_{AB} \frac{(1-B)}{(1-B)+K_{AB}} - Ck'_{CB} \frac{B}{B+K'_{CB}} \\ \frac{dC}{dt} &= Bk_{BC} \frac{(1-C)}{(1-C)+K_{BC}} - Ak'_{AC} \frac{C}{C+K'_{AC}}\end{aligned}$$



If the first (activation) reaction on B is saturated and the other linear, $A^* = B^* C^* k'_{CB} / k_{AB} / K'_{CB}$.

Substituting it into the third equation at steady state, we have

$$k_{BC} \frac{(1-C^*)}{(1-C^*)+K_{BC}} - \frac{C^* k'_{CB}}{k_{AB} K'_{CB}} k'_{AC} \frac{C^*}{C^* + K'_{AC}} = 0$$

C^* is a constant independent of the input.

Supplemental References:

- Ciliberto A, Capuani F, Tyson JJ. Modeling networks of coupled enzymatic reactions using the total quasi-steady state approximation. *PLoS Comput Biol.* (2007) **3**:e45.
- Gomez-Uribe C, Verghese GC, Mirny LA. Operating regimes of signaling cycles: statics, dynamics, and noise filtering. *PLoS Comput Biol.* (2007) **3**:e246.
- Tzafriri AR. Michaelis-Menten kinetics at high enzyme concentrations. *Bull Math Biol.* (2003) **65**:1111.

Supplemental Figure Legends:

Figure S1. The probability plot for all the 81 two-node networks. The networks are composed of the input node A and the output node C. None of them are capable of adaptation.

Figure S2. The probability plot for all the 36 networks with 3 nodes and 2 links. None of the 3-node networks with less than 3 links are capable of adaptation.

Figure S3. The probability plots for each of the 3-node 3-link networks that contain either one feedback or feed-forward loop between different nodes.

Figure S4. Adaptation networks studied in our enzymatic model are also capable of adaptation under inputs of the multiple up/down steps. Two examples are shown here: a single negative feedback loop (upper panel) and a single incoherent feed-forward loop (lower panel).

Figure S5. Selection criterion for excluding circuits with damped oscillations.

Figure S6. Phase diagram and nullclines for a single negative feedback loop with (upper panel) and without (lower panel) the buffer node. The solid lines are nullclines corresponding to the initial input and the dashed to the changed input.

Figure S7. Motif analysis of 395 robust adaptation networks. Significance is shown for each feedback of feed-forward loops as motifs.

Figure S8. Phase diagrams and nullclines of a network with one negative feedback loop and one positive self-loop on B. The B-nullcline ($dB/dt=0$) is drawn in black line and C-nullcline in red (solid red for the initial input and dashed red for the changed input). The change of K_{BB} is from 1 to 0.02; K'_{CB} from 1 to 10; k_{BC} from 1 to 100; and k'_{AC} from 1 to 100.

Figure S9. The B-regulation and the corresponding B-algebra in NFBLB networks (two left columns). Shown in the next column is the number of networks among the 395 robust adaptation networks that implement the regulation. An example network in each case is shown on the right.

Figure S10. The B-regulation and the corresponding B-algebra in IFFLP networks (two left columns). Shown in the next column is the number of networks among the 395 robust adaptation networks that implement the regulation. An example network in each case is shown on the right.

Figure S11. An example network (upper panel) that cannot achieve perfect adaptation but appears to be robust (large Q -value). The network contains an incoherent feed-forward loop but its regulation on B does not belong to any of the B-regulations of IFFLP class (Figure S9). When the grey link is removed, the resulting network (lower panel) is more robust and its B-regulation is in the list of the IFFLP class shown in Figure S9.

Figure S12. A network (left) with a coherent FFL. With a self-loop on B, this coherent FFL can function like an incoherent FFL. A negative FBL (between B and C) is necessary to make the relevant steady state stable. Removing the link from A and B, the resulting network (right) is more robust.

Figure S13. Mass action reaction models for three typical adaptation networks. A) Network with negative feedback loop. B) Network with incoherent feed-forward loop. C) Network with negative feedback loop and a positive self-regulation on node B. The left are the Michaelis-Menten (MM) models used in the main text, the middle are the mass action reaction models used for simulation here. Certain nodes in the MM model are expanded in the mass action reaction models by adding an additional node D (pink region) to avoid titration by its substrate. The right side figures are simulation results using mass action reaction models. All the key regulations are colored with orange (saturated) or blue (linear).

Figure S14. Comparison of robustness Q with different sample size and cutoff. A) Comparison of the robustness Q when using 1,000 and 10,000 samples of parameter sets. B) Comparison of the robustness Q when using different cutoffs for precision and sensitivity.

Figure S15. The design table of 3-node enzymatic networks for perfect adaptation. Starting with simple adaptation networks, additional negative feedback loops that (1) go through B, (2) do not violate the adaptation mechanism, and (3) do not result in any positive feedback loops are added, until no more such loops can be added. The Q -value was obtained from sampling 10,000 parameter sets, and the number in parenthesis is the Q -value from sampling 100,000 parameter sets. Green arrows indicate an increase in Q with additional loops, red arrows indicate a drop in Q , and black arrows indicate no detected changes in Q . In all the cases of decreasing Q the number of parameters is increased with the additional loop.

All possible 2-node networks (81)

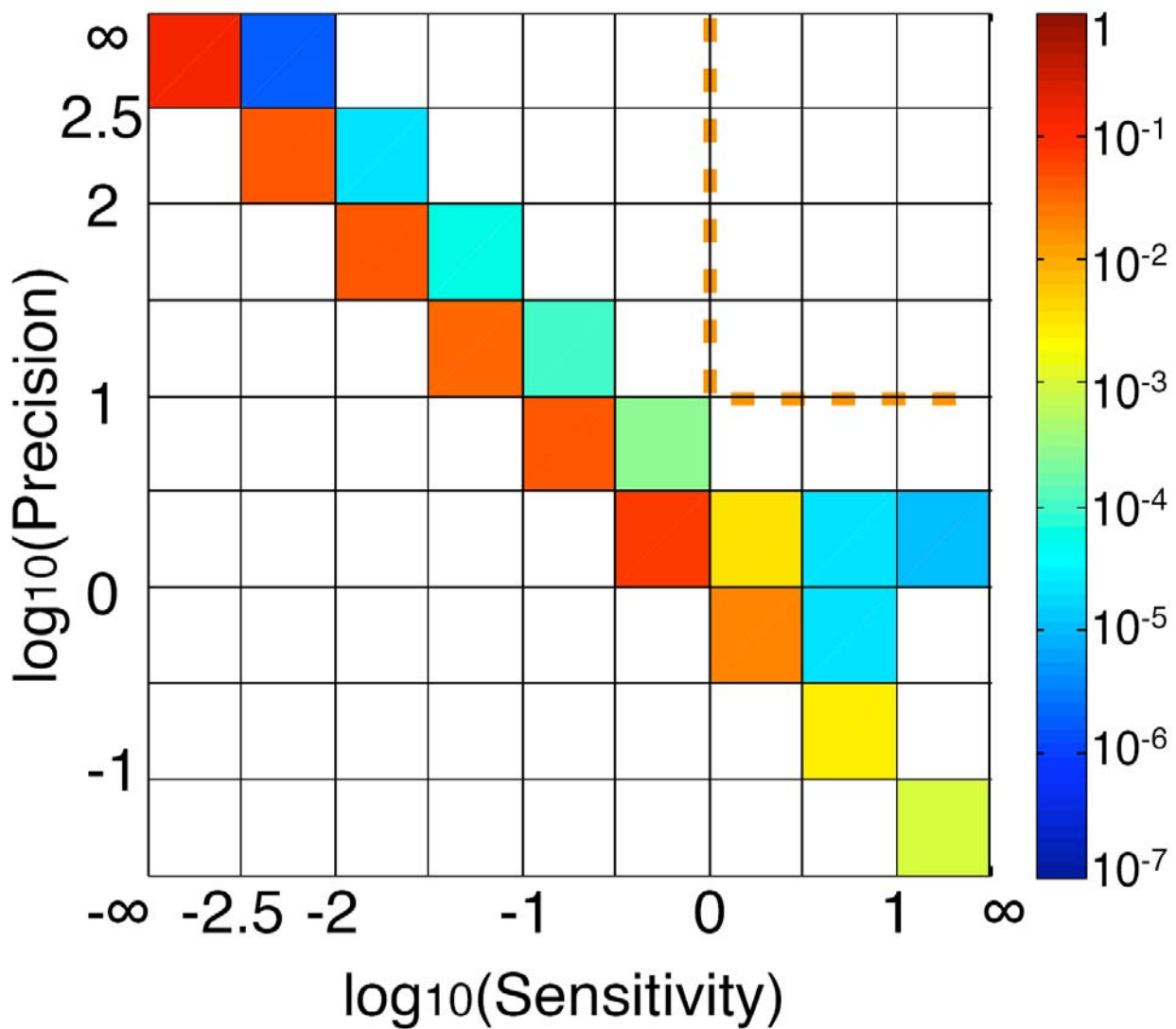


Figure S1

All possible 3-node 2-link networks (36)

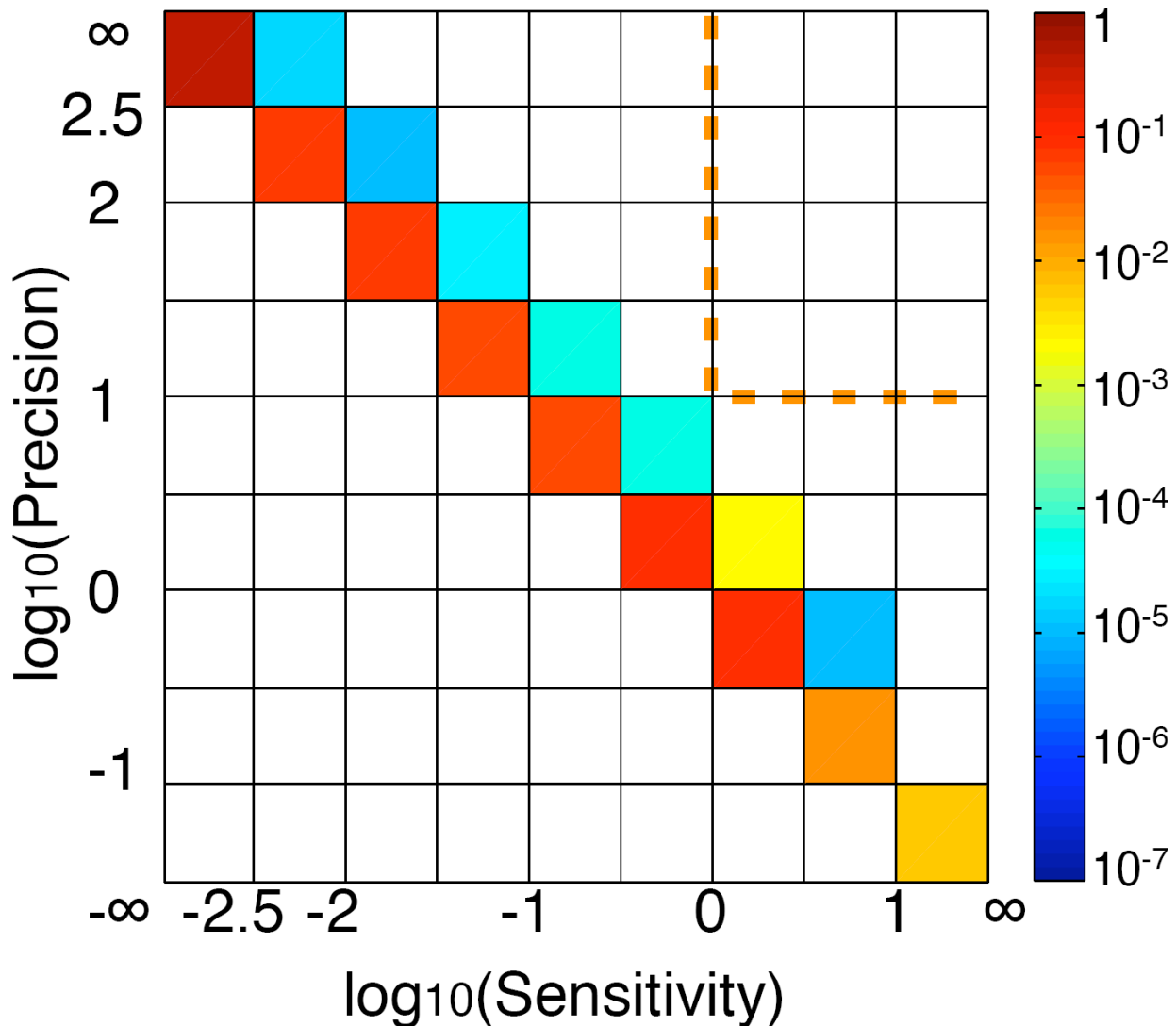


Figure S2

All possible 3-node 3-link networks with one feedback or feed-forward loop (40)

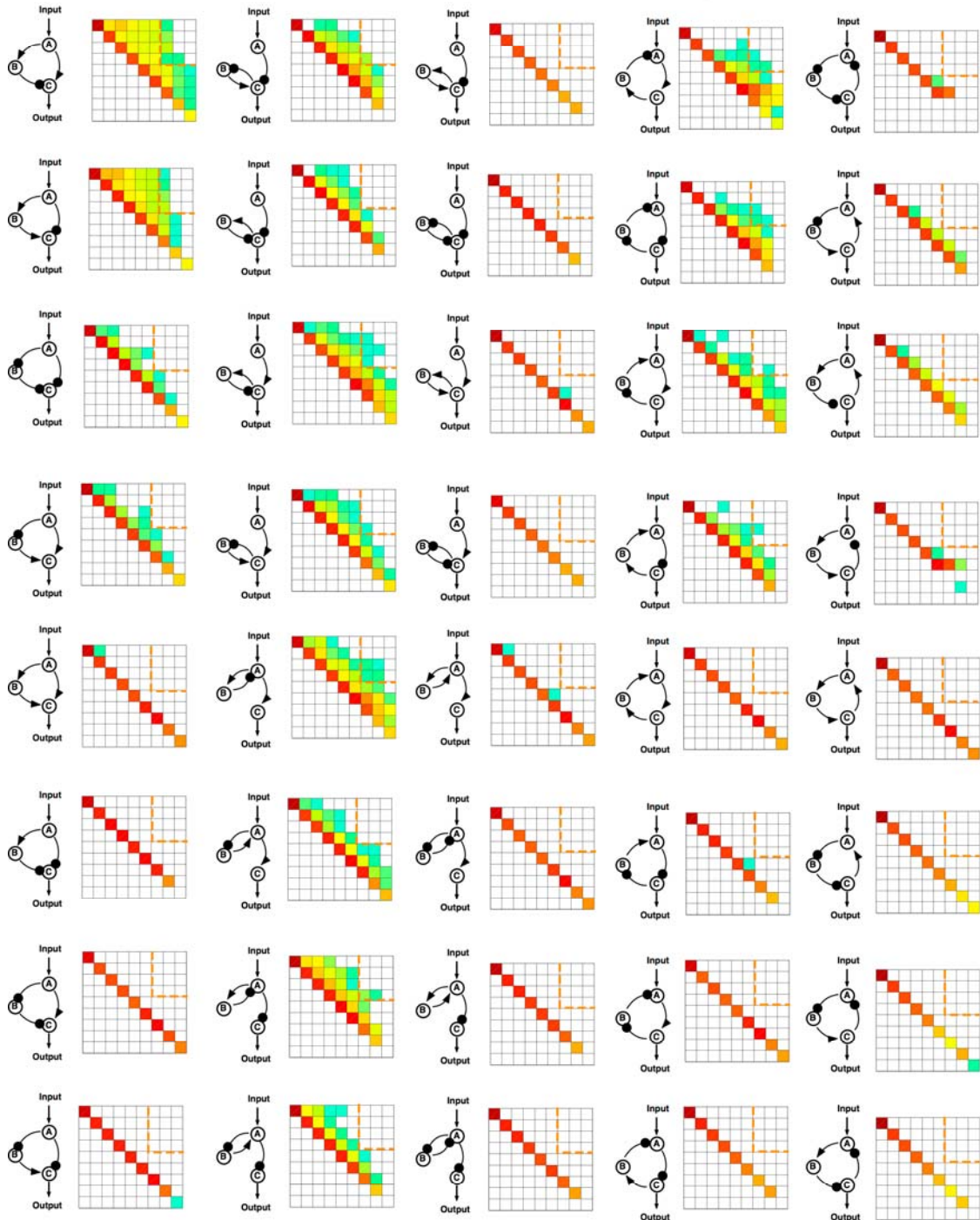


Figure S3

Response to multi-step inputs

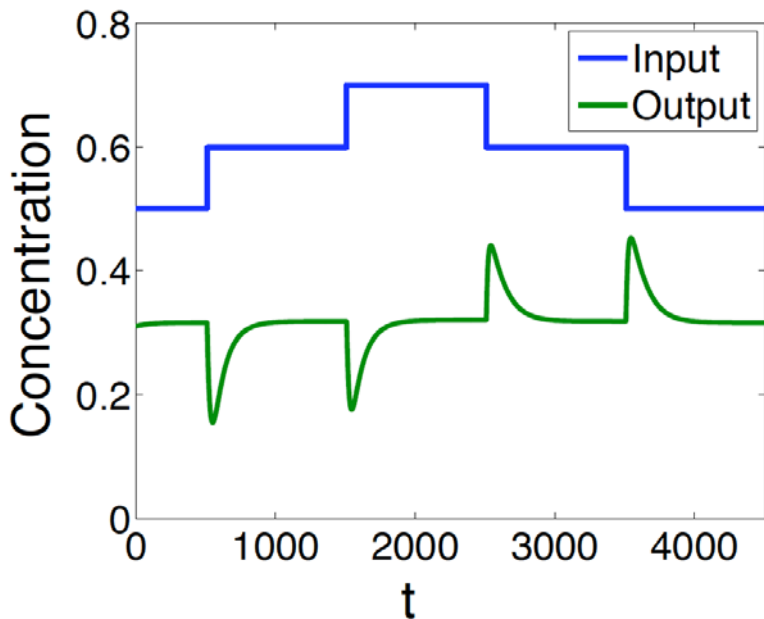
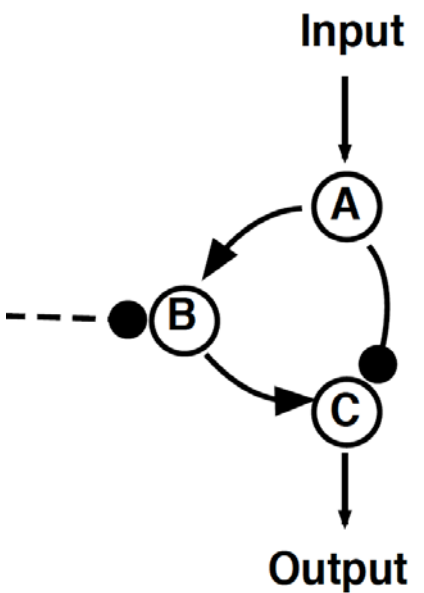
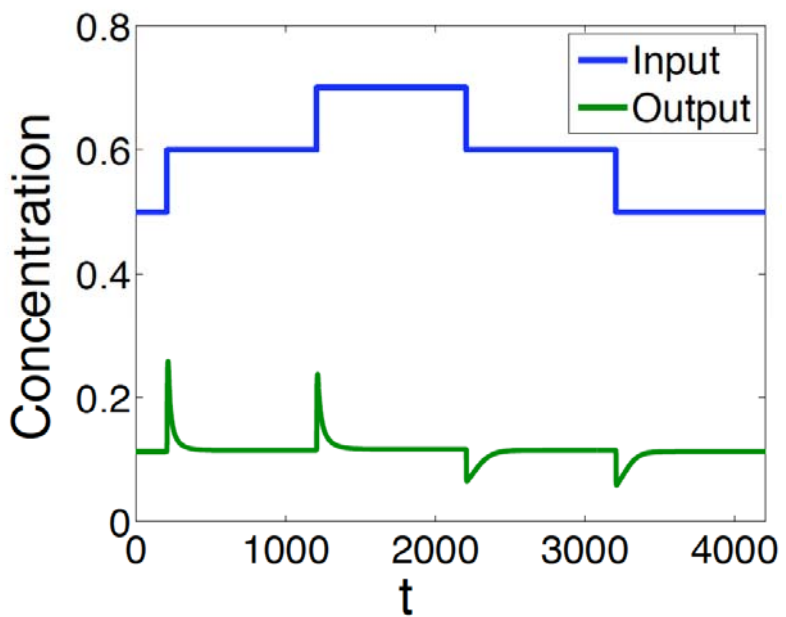
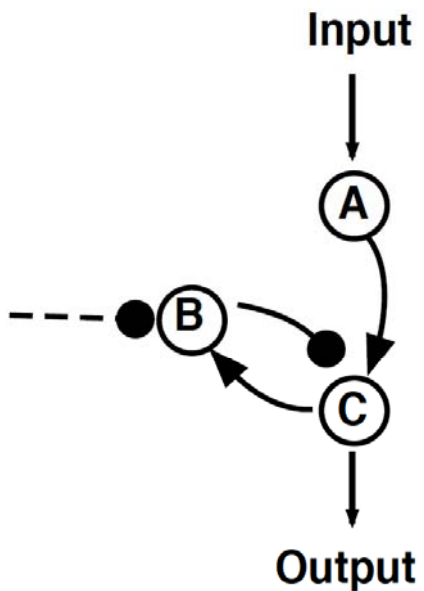


Figure S4

Criterion for excluding damped oscillation

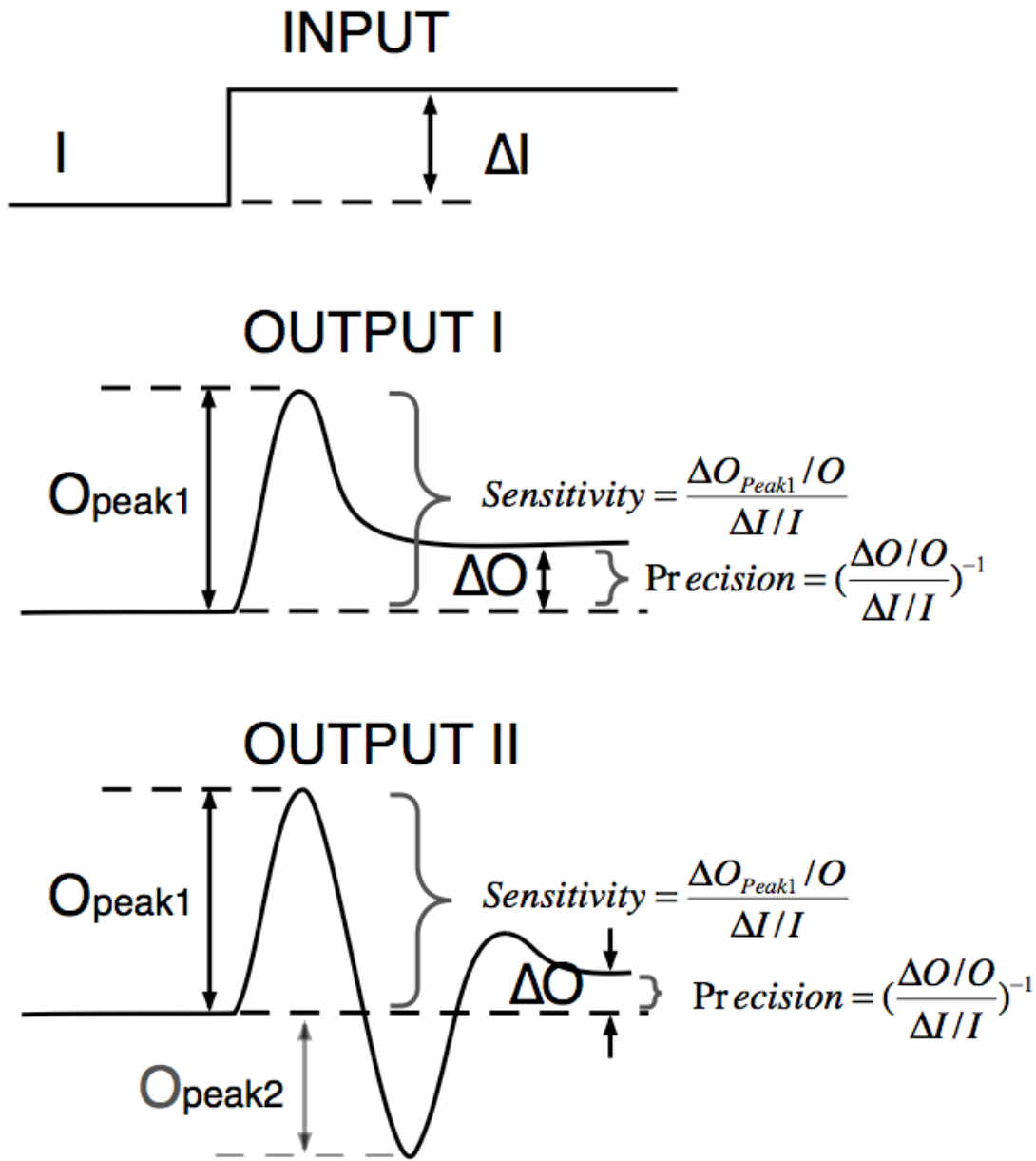


Figure S5

Negative feedback loops with and without buffer node

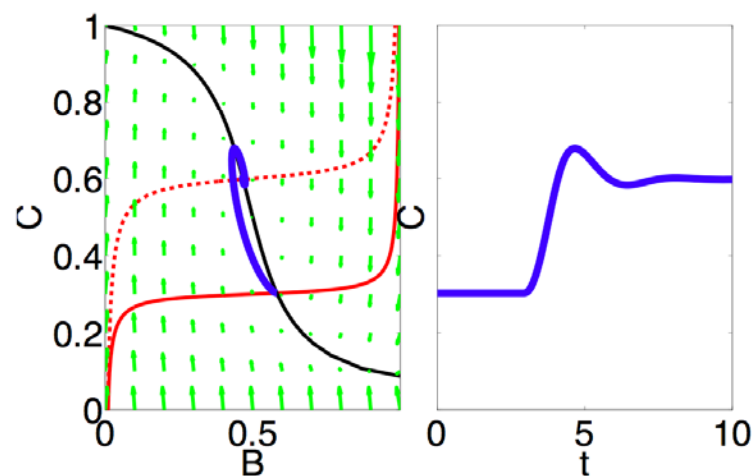
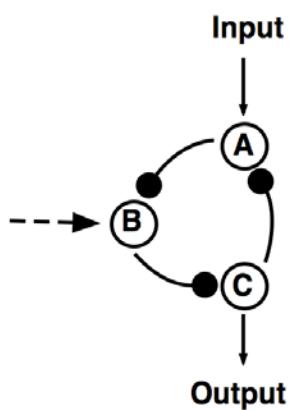
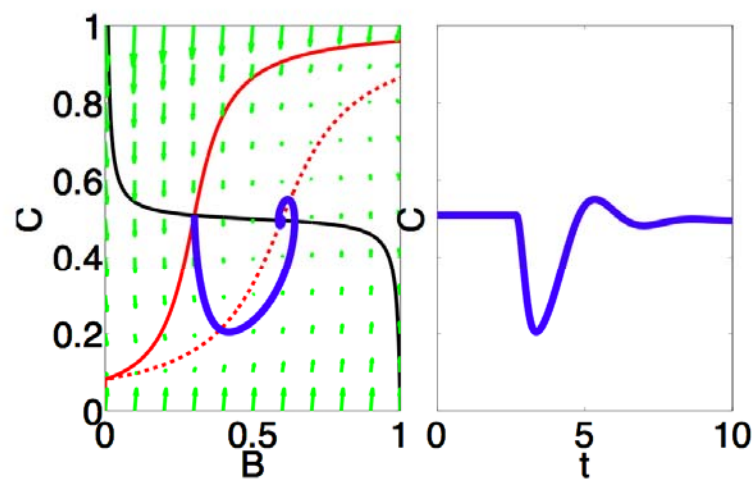
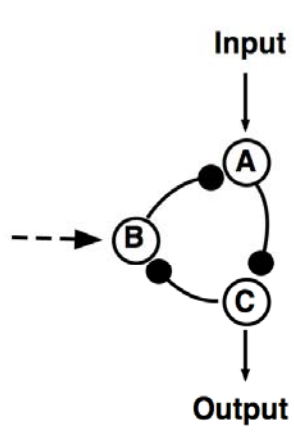


Figure S6

Motif analysis of 395 robust adaptation networks

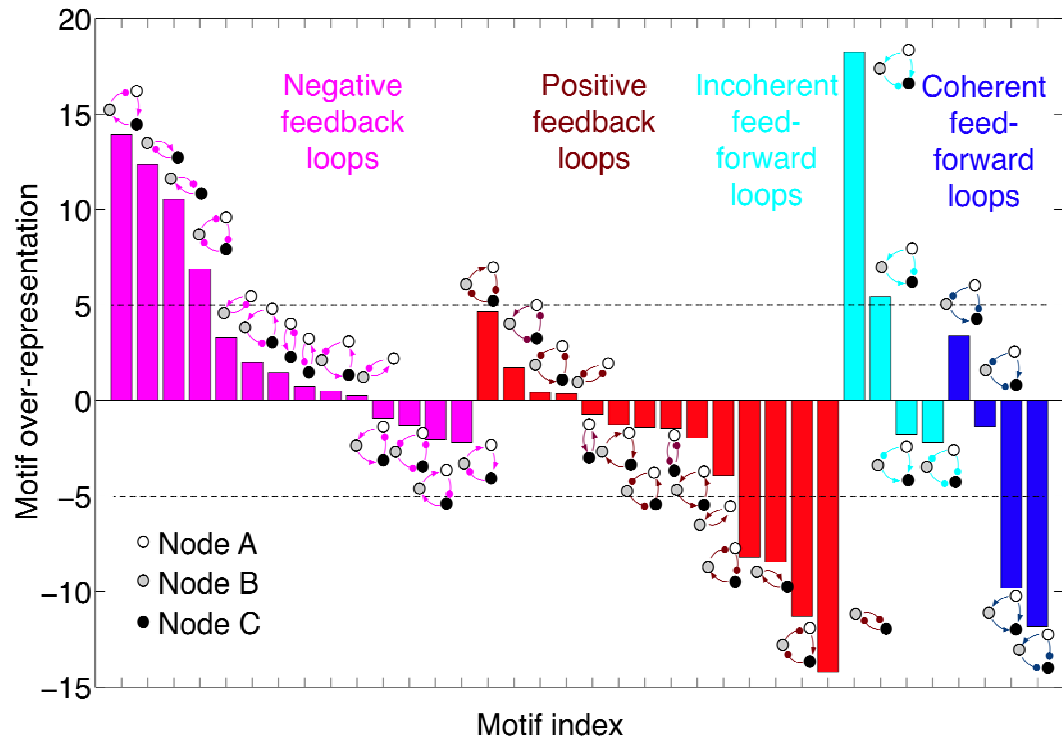


Figure S7

Control reactions/parameters of NFBBLB with a positive self-loop on B

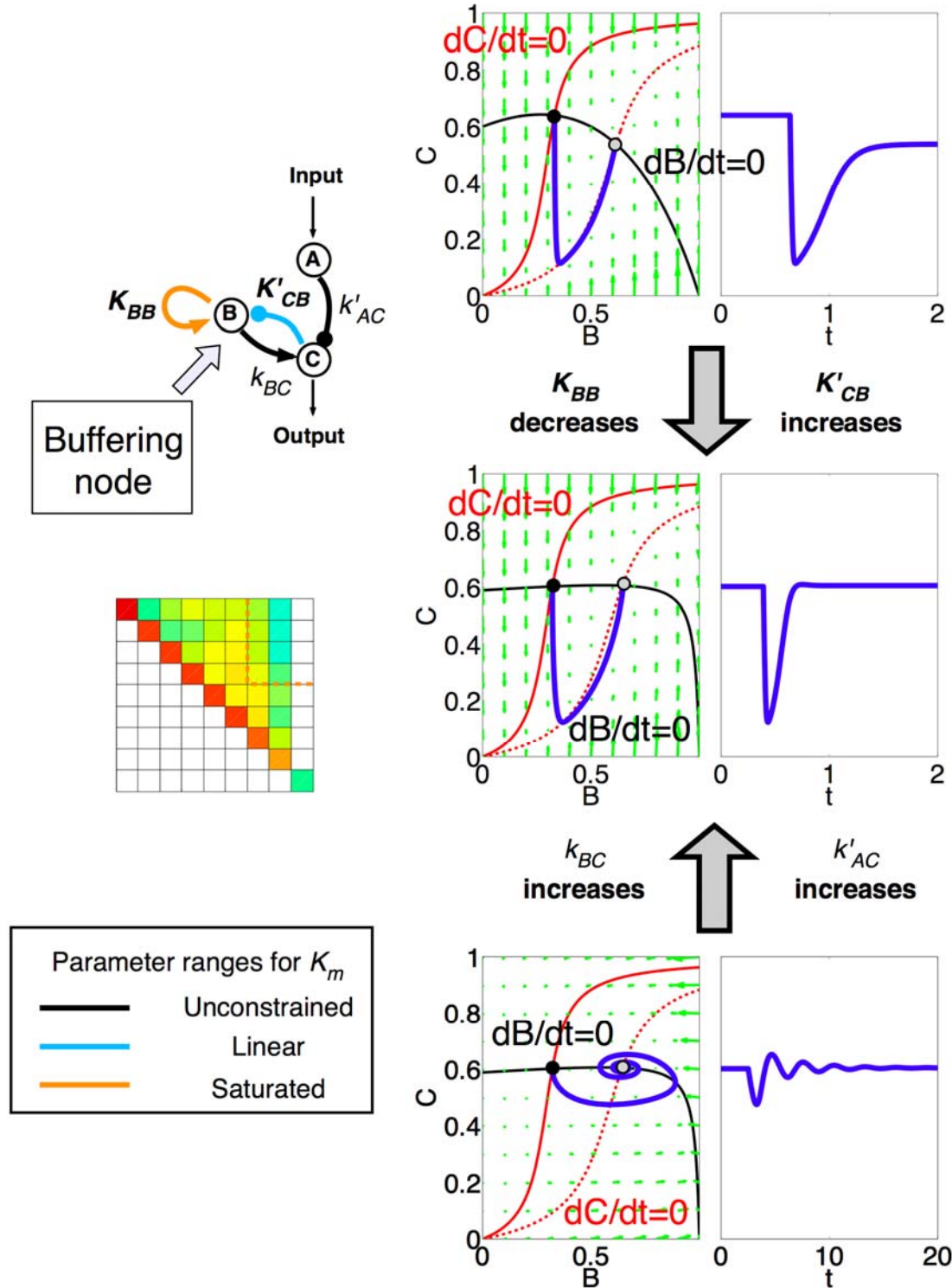


Figure S8

B-algebra for NFBLB class

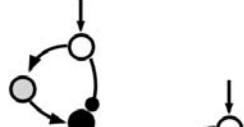
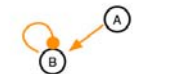
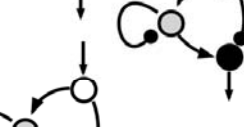
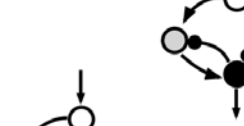
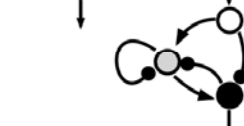
B-regulation	B-algebra	Number of robust networks in the class	Example
	$A^* = \text{constant}$	0	
	$A^* = \text{constant}$	0	
	$C^* = \text{constant}$	14	
	$C^* = \text{constant}$	10	
	$\alpha A^* + \gamma C^* + \delta = 0$	2	
	$\alpha A^* + \gamma C^* + \delta = 0$	0	
	$A^* \propto C^*$	21	
	$A^* \propto C^*$	0	
	$A^* = \text{constant}$	1	
	$C^* = \text{constant}$	100	
	$\alpha A^* + \gamma C^* + \delta = 0$	13	

Parameter ranges for K_m

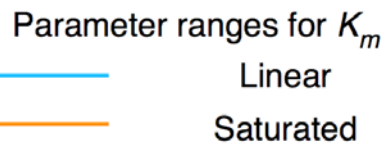
- Linear
- Saturated

Figure S9

B-algebra for IFFLP class

B-regulation	B-algebra	Number of robust networks in the class	Example
	$A^* \propto B^*$	59	
	$A^* \propto B^*$	14	
	$A^* \propto B^*$	9	
	$A^* \propto B^*C^*$	59	
	$A^* \propto B^*F(C^*)$	23	
	$A^* \propto B^*F(C^*)$	33	

Parameter ranges for K_m



Linear

Saturated

Figure S10

Violation of B-algebra compromises robustness

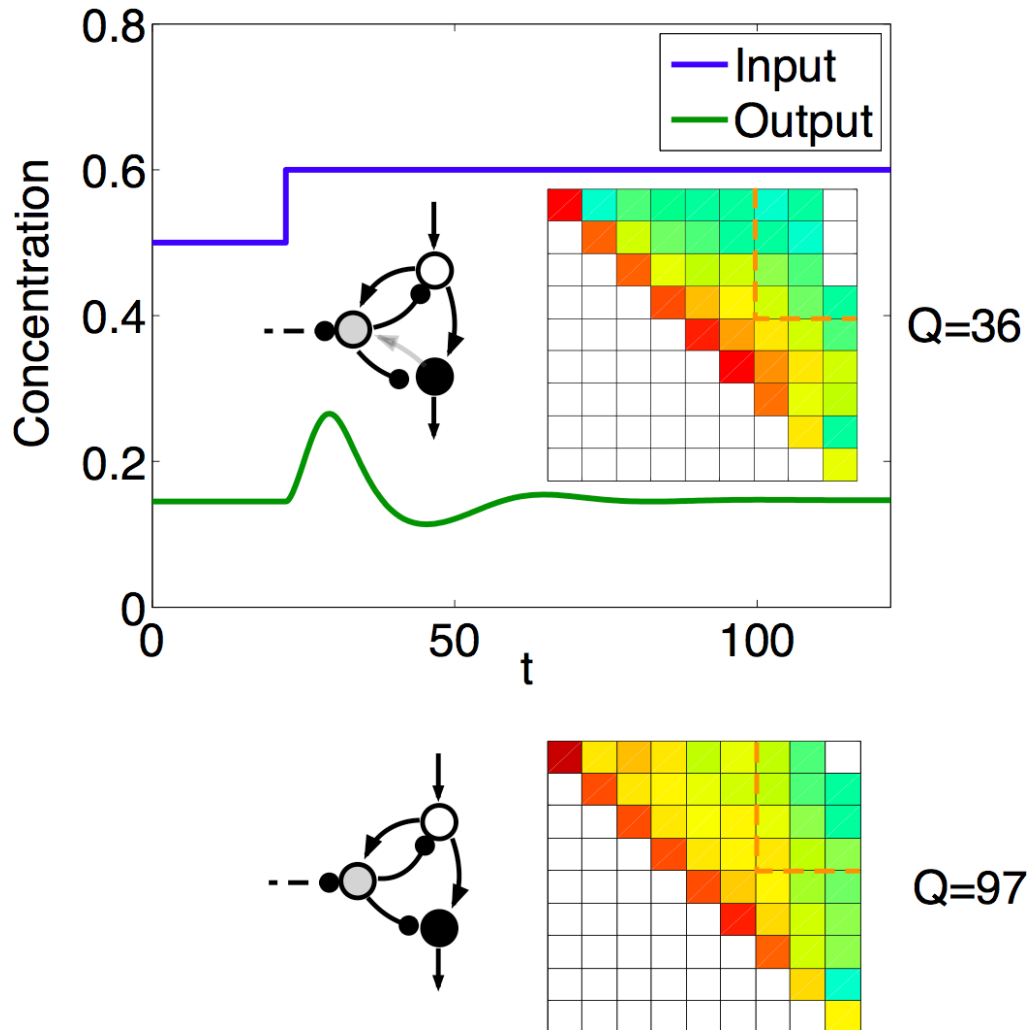


Figure S11

A special kind of coherent FFL behaves like IFFL

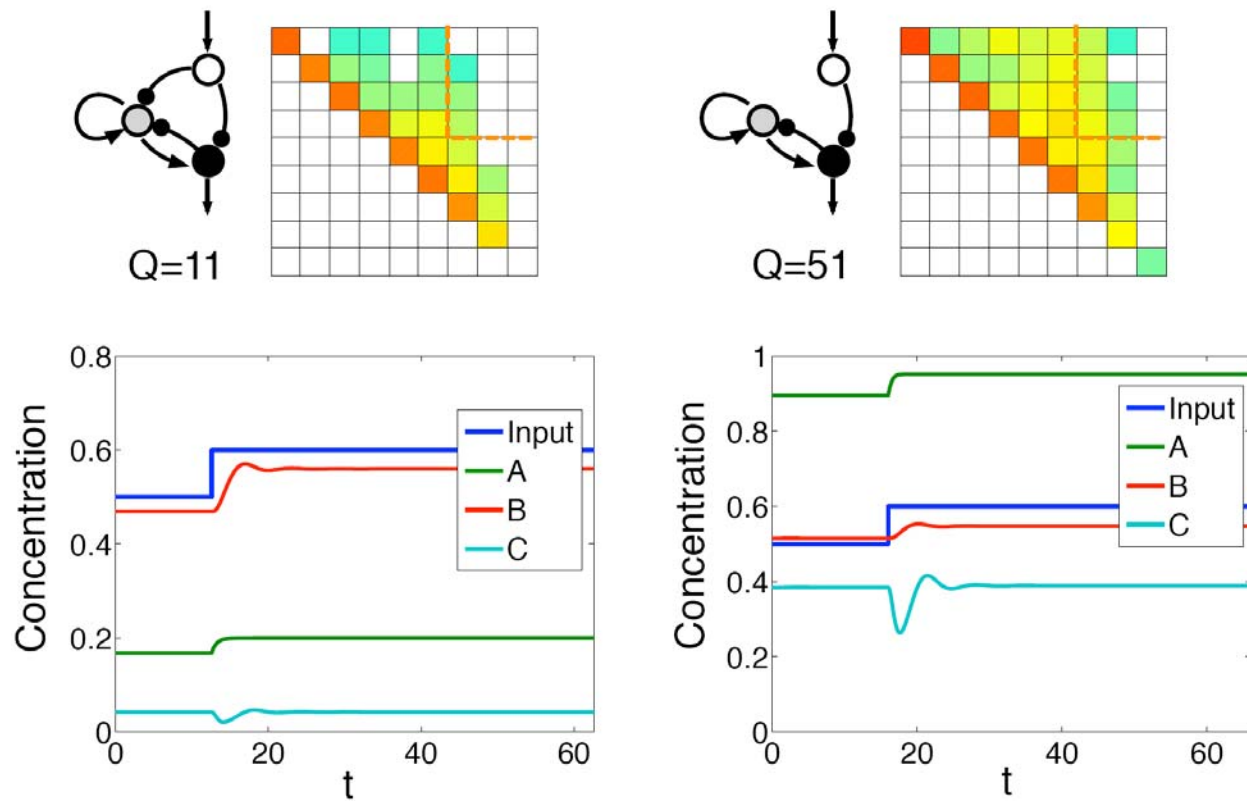


Figure S12

Mass action reaction models

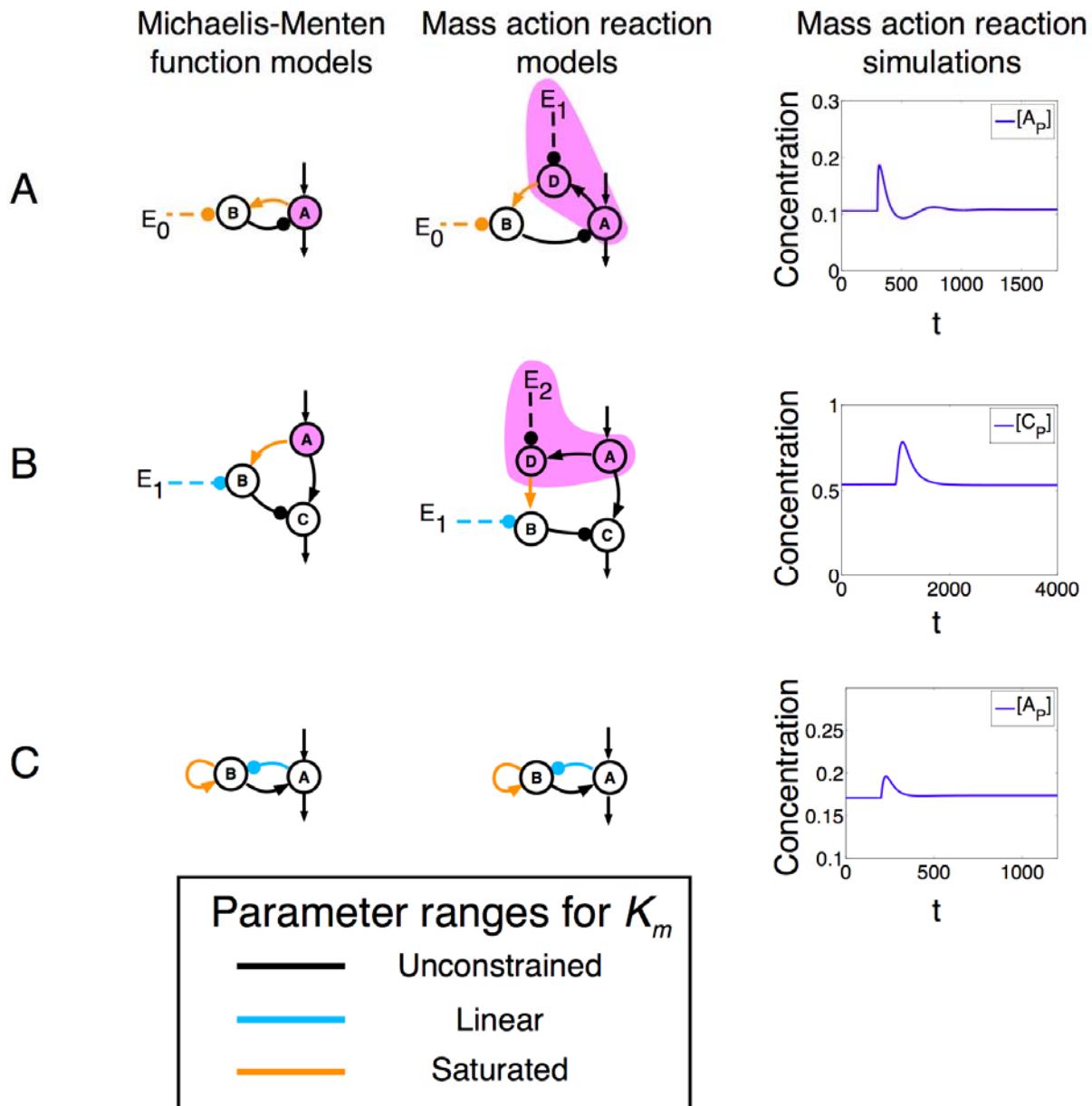


Figure S13

Comparison of different sample size or presicion/sensitivity cutoff

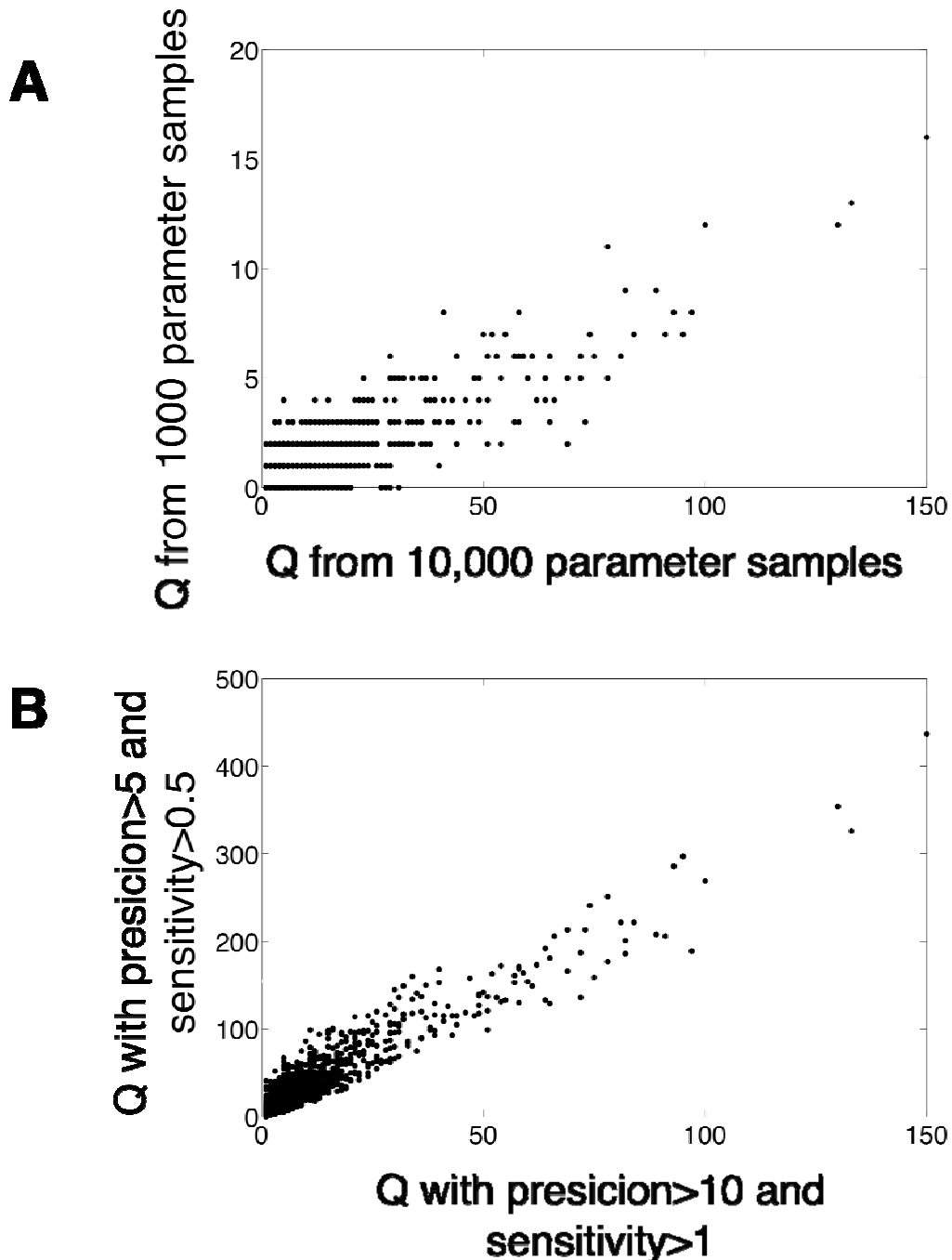


Figure S14

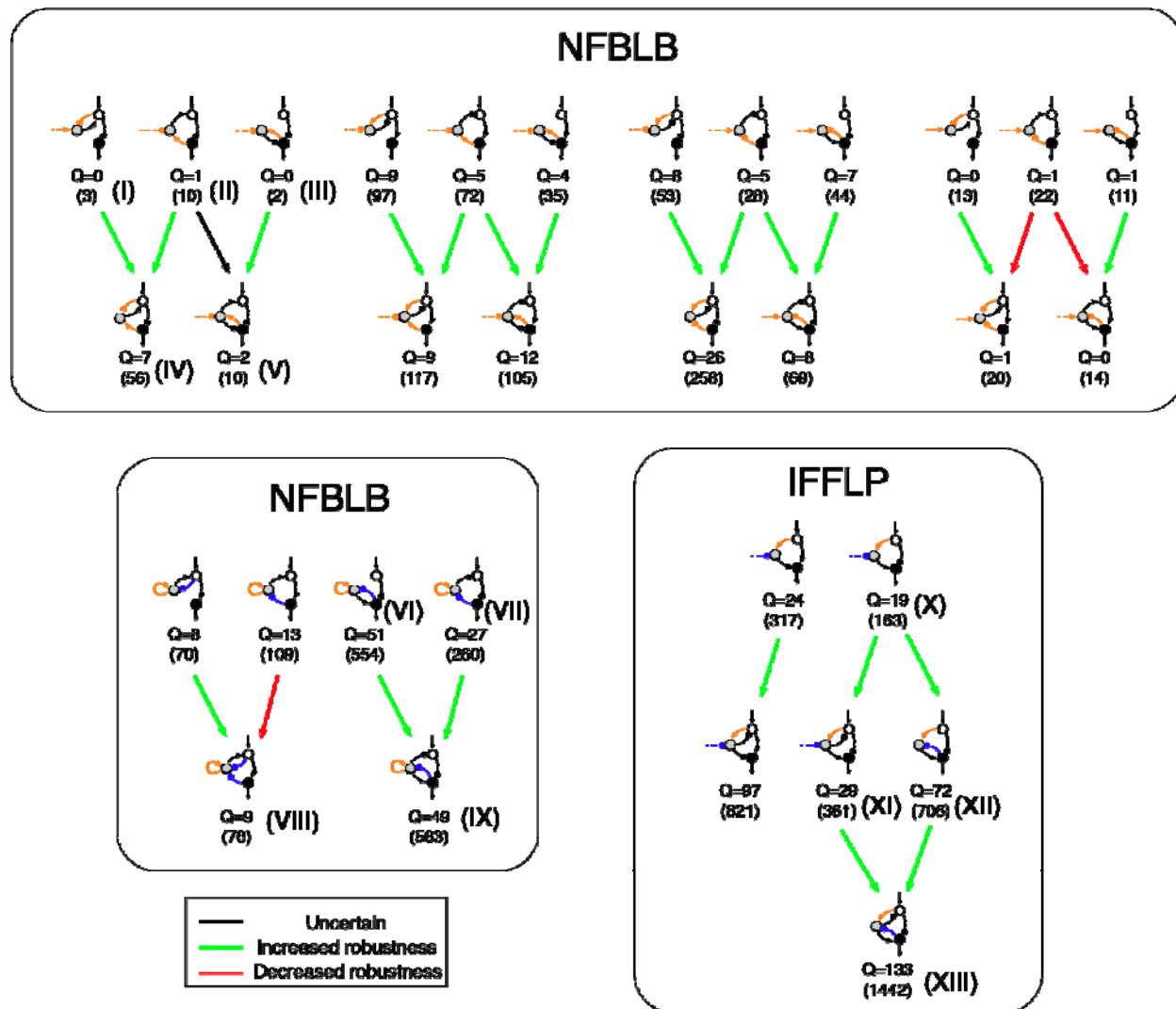


Figure S15